

# Weathering the Storm: Supply Chains and Climate Risk

Juanma Castro-Vincenzi \*

Gaurav Khanna †

Nicolas Morales‡

Nitya Pandalai-Nayar§

February 2024

## Abstract

We characterize how firms structure supply chains under climate risk. Using new data on the universe of firm-to-firm transactions from an Indian state, we identify firms exposed to climate risk through their supply chains. Using an event-study design we find firms with suppliers districts that flooded experienced a decline in inputs of 75% that persisted 2 months. Affected firms returned to their original suppliers after the shock. We develop a general equilibrium model of firm input sourcing under climate risk. Firms diversify otherwise identical inputs from suppliers across space, trading off the probability of a climate shock against the cost of higher inputs. We quantify the model using data on 271 Indian districts. The model implies expected real wages vary across space and are correlated with geography, productivity and climate risk. The volatility of real wages is 84% lower under sourcing with climate risk compared to autarky. While expected real wages are 11.6% lower in autarky overall, for 5% of districts expected real wages are higher under autarky as diversification for these districts comes with higher cost inputs. Diversification through supply chains unambiguously lowers the volatility of real wages, but can have positive or negative effects on their level.

*JEL:* F14, L14

*Keywords:* Production networks, supply chains, firm dynamics, climate change

---

\*Harvard University, jcastrovincenzi@fas.harvard.edu

†University of California, San Diego, gakhanna@ucsd.edu

‡Federal Reserve Bank of Richmond, nicolas.morales@rich.frb.org

§University of Texas, Austin and NBER, npnayar@utexas.edu

We thank Claire Conzelmann and Simon Farbman for outstanding research assistance and Swapnika Rachapalli for sharing inventory data. We also thank seminar and conference participants at Michigan and Kiel-CEPR Geopolitics Conference for helpful comments. The views expressed are those of the authors and do not necessarily reflect those of the Federal Reserve Bank of Richmond or the Board of Governors.

# 1 Introduction

The intersection of complex supply chains and climate risk presents a critical challenge to the global economy. While complex supply chains have yielded significant efficiency gains worldwide, enabling firms to procure inputs from the most efficient suppliers regardless of their location, escalating climate risk raises concerns about the vulnerability of global production networks and the ensuing broader economic fragility (Barrot and Sauvagnat, 2016; Boehm et al., 2019). Increasing global risk of climate change also heightens the likelihood of natural disasters such as flooding and storm surges. In response, forward-looking firms may choose their production locations (Castro-Vincenzi, 2024) or diversify the locations of their suppliers based on geographic variability in climate threats, to mitigate the impact of disruptions to their productive activities. Therefore, our understanding of how climate change may reshape economic production and its implications for welfare across regions hinges on firms' adaptive sourcing decisions in response to escalating hazards. In this paper, we provide a theoretical, empirical, and quantitative analysis of the spatial consequences of supply chain restructuring in light of increased climate risk.

Studying the general equilibrium consequences of how firms structure supply chains when faced with climate hazards raises two important challenges. First, for empirical evidence on how firms respond to climate risk, we need high-frequency data on transactions along the supply chain, the precise locations of establishments, and meaningful variation in weather-related events. Second, to quantify the broader economy-wide consequences, we require a general equilibrium model of firm input sourcing under climate risk, where firms face trade-offs such as lower probability of climate shocks against higher-cost, less productive inputs or higher shipping costs.

To address the first challenge, we obtain the universe of establishment-to-establishment level transactions from a large state in India, as long as one node of the transaction (either buyer or seller) is in the state (the other node can be anywhere in the country). This dataset contains the precise zip code of the establishments, the value of the transaction, the product code, the date, the quantity (and so the unit values), and the unique tax ID of the establishment. Using these data, we document important new facts suggesting firms are optimizing supply chains to mitigate climate risk. First, firms diversify the locations they source from, even within narrow product codes. And second, firms that multi-source the same product buy from farther distances and dryer regions.

A key advantage of our setting is that India experiences monsoonal rainfall that follows a somewhat predictable spatial pattern every year, although the intensity and timing can vary. Regions across India are regularly and increasingly experiencing large flooding events that disrupt firm supply chains. Firms operating in this environment might reasonably

take into account the probability of climate-related disruptions to their operations, as hinted at in our descriptive analysis.

To provide causal evidence of firm responses to climate shocks, we leverage the exogenous geographic and temporal variation in flooding events using a staggered event study design. We show that the sales of flood-hit suppliers fall drastically over three months, but recover by five months after a flood. Further, the total purchases of downstream buyers decrease substantially, and they are unlikely to substitute to other suppliers. Yet, we detect no change in the sales of these downstream buyers. Prices increase in the short run, but once again recover. Importantly, we show no difference in affected and unaffected firms in the pre-period. Our descriptive and event-study results together suggest firms plan for climate-related risk and recover from the realized shocks relatively quickly. These empirical patterns motivate and discipline our general equilibrium framework.

In addressing the second challenge of quantifying economy-wide impacts, we introduce a new theory. We build a spatial general equilibrium model of firm sourcing under climate risk. Motivated by our empirical results and the patterns in the data, firms diversify their sourcing of otherwise identical inputs across locations to mitigate climate risk. Such diversification comes with a trade-off: places with lower climate risk might be less productive, or geographically distant, necessitating payment of higher trade costs.

A key feature of the model is that firms' expected profit functions in the presence of sourcing risk are concave in input orders. That is, firms behave as if they are risk averse, even in the absence of explicit risk aversion in preferences. This implies that firms from each region will choose to diversify their input sourcing across regions if they face heterogeneous shock probabilities, even in the extreme case where regional fundamentals are constant across space, and trade is costly (a "symmetric" economy). In a comparative statics exercise, we show that in this setting, there might be no conventional gains from trade, but trade still occurs purely due to the diversification motives of firms. As a result, despite identical fundamentals, "safer" regions see higher real wages in general equilibrium, while more distant or riskier regions see lower real wages.

Interestingly, this comparative statics exercise implies that the prices of inputs and, therefore, of regional consumption are higher under costly trade than regional autarky. A stark insight from this exercise is that the average expected regional real wage is lower under costly trade than under autarky, but its volatility is also lower.<sup>1</sup> In other words, under commonly used consumer preferences that do not explicitly have a role for the volatility of real wages in welfare, costly trade is welfare decreasing. We show, however, that free trade in the symmetric economy brings both the diversification benefits of lower wage

---

<sup>1</sup>Caselli et al. (2019) show that diversification across sectors can lower aggregate volatility in a quantitative trade model.

volatility and higher expected real wages compared to costly trade.

We quantify this model using a census of manufacturing firms across the country, allowing us to estimate location-specific productivities and labor shares. We implement the model on 271 districts in India. Our model implies that bilateral sourcing shares are a function of all regional labor endowments, productivities, and bilateral trade costs, as well as the risk of sourcing in each region. Given estimates of regional labor, productivity, and bilateral trade costs, we back out model-implied regional risk that is necessary to fit observed sourcing shares. To validate our framework, we project the model-implied risk on climate observables such as rainfall and flood events as well as other risk-related variables such as court capacity to capture institutional features that might affect firm decisions. We obtain a high partial  $R^2$  for the climate-related variables, suggesting firms are indeed taking into account climate risk in their supply chain decisions. The total  $R^2$  suggests that firms take into account several sources of risk when forming their supply chains, a feature that has been largely ignored by the literature (an exception is [Kopytov et al. \(2021\)](#) who study how supply chains adapt to supplier volatility).

While the comparative statics exercises provide stark analytical insights, the effects of firm diversification in a realistic economy will, in general, depend on the variation in fundamentals and “standard” motives for trade, such as geography and productivity in addition to risk-mitigation incentives. Our third contribution is, therefore, quantitative: we compute expected real wages across districts in our calibrated model, given model-implied sourcing risk. Our framework implies that as a result of firm sourcing decisions, real wages in each district will depend on the geography, productivity, and climate risk of all districts.

We perform several quantitative exercises in our calibrated model. First, we validate the insights from our comparative statics exercises. We find that under the estimated trade costs and climate risk, the variance of real wages is 86% lower. On the other hand, expected real wages do not always have to be lower than in autarky. In our calibrated model they are on average 11.6% higher, although 5% of districts do see expected real wages that are lower than autarky. We then study how regional wages change in general equilibrium under alternative shock probabilities, to capture scenarios of changing climate risk and highlight our new channel. Our model and quantification show that firm sourcing decisions help mitigate the effects of climate shocks, and have quantitatively important implications in general equilibrium for real wages in safer regions relative to riskier ones.

**Related literature** A growing literature studies how climate change shapes economic activity. Several papers focus on the long run, assessing how the distribution of economic

activity might change within and across cities, regions, and countries (e.g., Desmet et al. 2021, Nath 2022, Jia et al. 2022, Cruz and Rossi-Hansberg 2023, Hsiao 2023, and Bilal and Rossi-Hansberg 2023). A smaller subset considers optimal medium-term policy responses (Balboni, 2021). Another branch of the literature studies the effects of extreme weather events on firms' employment and location decisions, as well as on FDI (Castro-Vincenzi, 2024; Gu and Hale, 2022; Indaco et al., 2020; Pankratz and Schiller, 2021). In this paper, we study the general equilibrium impacts of endogenous firm supply network decisions under climate risk. While our emphasis is on how firms can use their supply networks to mitigate the risk of extreme weather events, our model is well suited to analyze the general equilibrium effects of supply network formation under any location-specific risk.

While the responses of firm supply chains to climate risk have not received much attention in the literature, closely related to our paper is parallel work by Balboni et al. (2023) who study firm supply chains responses to flood events in Pakistan. While our empirical strategies are broadly similar, our data vary in that they contain information on establishment locations, detailed product codes, prices, and quantities, enabling us to estimate responses of a rich set of variables to shocks. Our model also studies sourcing decisions and supply chains that are formed in anticipation of shocks, delivers strong implications for how wages across space are shaped by regional risk, and can be used to infer the risk firms assign to different sourcing locations.

Supply chain fragility and resilience have received increased attention in the literature following the Covid-19 pandemic (Goldberg and Reed, 2023; Grossman et al., 2021; Khanna et al., 2022). Our firm-to-firm data are similar to those used by Khanna et al. (2022), but our identification strategy uses extreme weather events, and our emphasis here is on the adaptation of supply chains to climate risk and the general equilibrium consequences. Our empirical evidence indeed suggests that firm supply chain responses to climate-related risk vary qualitatively and quantitatively from their responses to an unanticipated, temporary shock like Covid-19.

Our theoretical and quantitative results are also related to the insights in Kopytov et al. (2021) who study supply chain adaptation to supplier volatility. Aggregate volatility decreases in openness to trade in our framework, as firms mitigate risk. However, expected real wages are lower under costly trade compared to autarky in our model. This parallels their result that aggregate output is also lower due to diversification away from volatile suppliers. We show, however, that eliminating trade barriers permits both expected real wages and aggregate volatility to be lower, maximizing the benefits of diversification.

Finally, we also build on a growing research agenda on how production networks respond to shocks. A long literature documents the importance of international trade in inputs

and studies the macroeconomic consequences of such trade (Antràs et al., 2017; Caliendo and Parro, 2015; Hummels et al., 2001; Johnson and Noguera, 2012, 2017; Yi, 2003). A strand of this literature has emphasized the transmission of natural disasters through trade and supply chain links (Barrot and Sauvagnat, 2016; Boehm et al., 2019; Carvalho et al., 2021). In contrast to studying the responses of firms or sectors to the incidence of shocks, we quantify the general equilibrium economy-wide consequences of firm supply chain adaption to the (changing) probability of shocks.

The rest of our paper is structured as follows. Section 2.3 outlines our data, shows descriptive patterns, and our event study analysis around flood events. Section 3 sets up the model, derives some analytical results, and performs comparative statics. Section 4 calibrates and quantifies the model. Section 5 contains the counterfactuals, and Section 6 concludes.

## 2 Empirical Approach

### 2.1 Data

**Firm-to-firm trade.** Our primary data source is daily establishment-level transactions.<sup>2</sup> These data are from the tax authority of a large Indian state with a fairly diversified production structure, roughly 50% urbanization rates, and high population density. Comparing this context to other contexts with firm-to-firm transaction data, we observe that the state has roughly three times Belgium’s population, seven times Costa Rica’s, and double Chile’s.

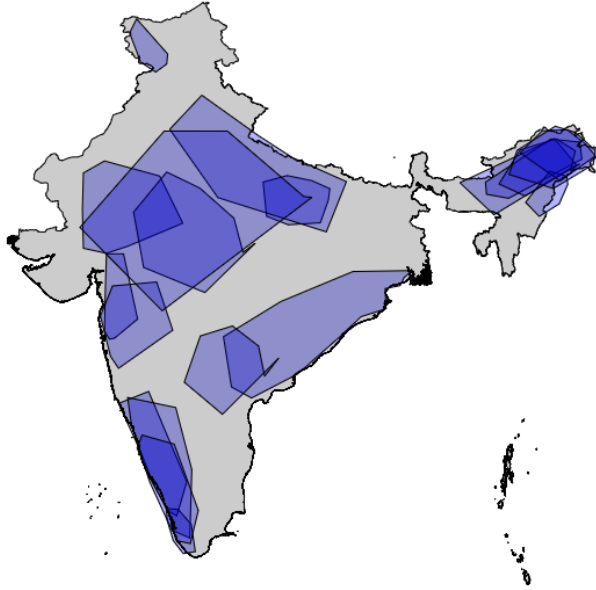
The data contain daily transactions from April 2018 to October 2020 between all registered establishments within the state, and all transactions where one node of the transaction (either buyer or seller) is in the state. All transactions have unique tax identifiers for both the selling and buying establishments, which include the value of the whole transaction, the value of the items being traded by 8-digit HSN code, the quantity of each item, its unit, and transportation mode.

Each transaction also reports the zip-code location of both the selling and buying establishments, which we merge with other geographic data. By law, any goods transaction with value over Rs.50,000 (\$700) has to generate eway-bills, which populate our data. Transactions with values lower than \$700 can also optionally be registered. As such, our network is representative of relatively larger firms, but the threshold is sufficiently low to capture small firms as well. More information is in Appendix A, with summary statistics in Table A1.

---

<sup>2</sup>While we use the term ‘firm’ in the paper, these data are at the granular establishment level.

Figure 1: Monsoonal Rain Floods, 2018-2020



Note: The figure plots the geographic coverage of all large floods that occurred between 2018 and 2020, as described in the Dartmouth Flood Observatory.

We use the data to construct the buyer-supplier network every period and the total value of inputs purchased and output sold by firms. To obtain a measure of real inputs and output, we use the reported quantity of each transaction to calculate unit values for each product, construct a price index and deflate the total firm-level input purchases and sales. Our output measure is noisier than inputs, given that we do not observe direct-to-consumer sales. Therefore, whenever using output as an outcome, we restrict the sample to firms with positive sales every period before the flooding event began.

**Climate data.** We use data from the Dartmouth Flood Observatory to identify geocoded flooding events throughout India. As shown in Figure 1, we identify 19 events of monsoonal rain throughout India between 2018 and 2021. For our main empirical analysis, we limit the set of floods to those that happen outside of our state, and that caused at least 100 individuals to be displaced due to the flood. These restrictions leave us with seven large flood events, which we use in our analysis in section 2.3.

We complement the climate-related datasets with information on daily rainfall by district, obtained from the India Meteorological Department (IMD).

## 2.2 Descriptive Analysis

To begin our analysis, we document three facts related to supplier diversification and climate risk to motivate the key features of our model.

**Fact 1: Even within narrow product categories, there is a significant mass of**

firms that source the same product from multiple regions.

We take advantage of the detailed product information in our transaction data and compute the number of districts a firm sources a given product from. As shown in Table 1 Column 1, 63% of the firms in our data buy from more than one district. In Columns 2 - 4 we show that a significant fraction of firms also multi-source the same product across regions. We compute the number of districts a firm - HSN product code pair sources from. In Column 2, we use 2-digit product codes; in Column 3, we use 4-digit product codes; and in Column 4, 8-digit product codes. Even with the narrowest product definition available in our data, 17.4% of firms source the same product from more than one district. This is evidence that a significant fraction of firms multi-source their products.

Table 1: Share of firms that source from multiple districts

Number of supplier districts	Share of buyers	Share of buyers x HSN 2	Share of buyers x HSN 4	Share of buyers x HSN 8
1	36.9%	65.8%	74.8%	82.6%
2	20.0%	16.2%	13.3%	9.7%
3	11.8%	6.4%	4.4%	2.3%
4	7.5%	3.1%	1.8%	0.8%
5	5.1%	1.7%	0.9%	0.4%
6	3.6%	1.1%	0.5%	0.2%
7	2.6%	0.7%	0.3%	0.1%
8	1.9%	0.4%	0.2%	0.1%
9	1.5%	0.3%	0.1%	0.1%
+10	9.2%	4.2%	3.7%	3.8%

*Note.* Column 1 aggregates the data at the firm-level and computes the share of firms that source from a certain number of districts. Column 2 aggregates the data at the firm - 2-digit product level, Column 3 at the firm - 4-digit product level and Column 4 at the firm - 8-digit product level.

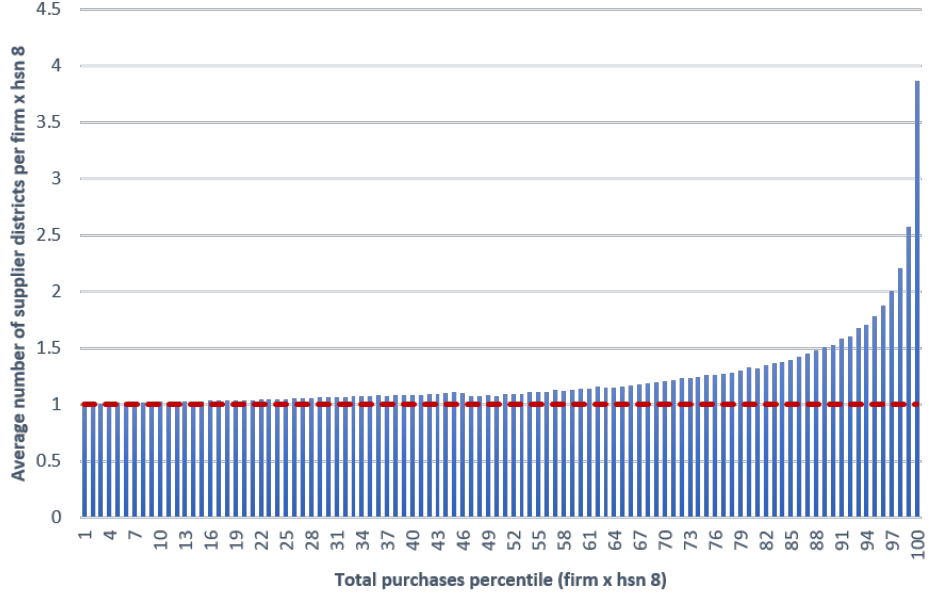
**Fact 2: Firms that have larger purchases of a given product are more likely to source from multiple regions.**

We rank all firm - 8-digit HSN pairs into percentiles, based on total purchases, where the higher percentiles include the firm-product pairs with the higher purchase volume. As shown in Figure 2, the smallest firm-product pairs tend to only source from a single supplier. However, towards the end of the distribution, the largest firm-product pairs source on average from more than one region. Firms above the 95th percentile source, on average, from two districts and firms in the top percentile source from four. This suggests that larger, more productive firms are more likely to multi-source.

**Fact 3: Firms that multi-source more tend to buy products from farther distances, slightly dryer regions, and pay higher input prices.**

Once again, we focus on firm-product pairs using the 8-digit product classification. In Figure 3a, we show that firms that source the same product from more regions, tend to

Figure 2: Number of supplier districts by total purchases



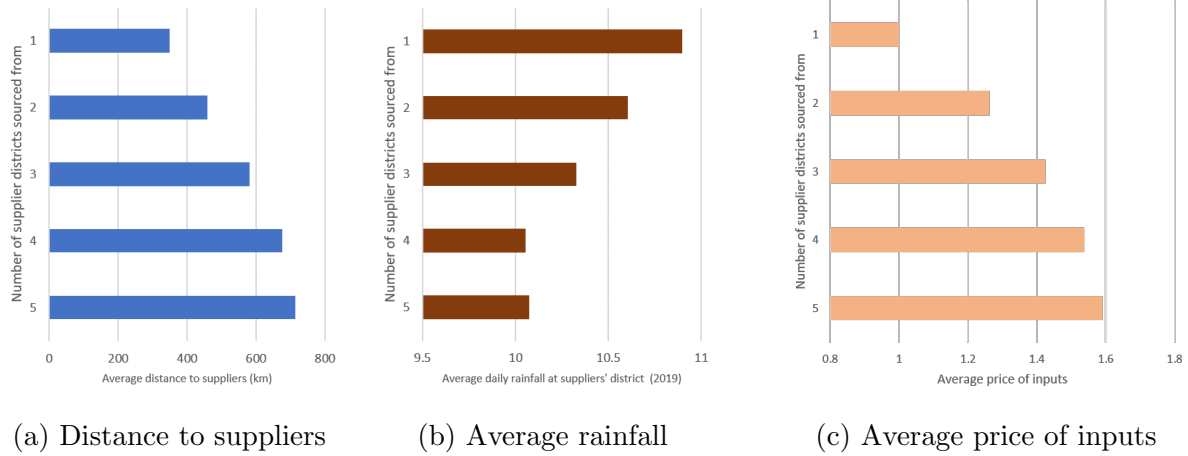
*Note.* We rank all firm-product pairs into percentiles (1-100) based on the volume of total purchases during 2019. For each percentile (in the horizontal axis), we compute the average number of districts the firm-product pairs source from.

buy from suppliers who are farther away. For instance, firm-product pairs that source from one district have an average distance to suppliers of 350 km. On the other hand, firm-product pairs with five suppliers per product have an average distance of almost double, at 700 km.

In Figure 3b, we also show that firm-product pairs with more suppliers also seem to source from less rainy districts. For firm-product pairs that source from one district, such districts have on average a 10.9 mm daily rainfall. On the contrary, for firm-product pairs that source from five districts, such districts have, on average, 10 mm of daily rainfall. The average daily rainfall across all Indian districts is 8.11 mm, so the difference between those sourcing from one vs five districts is 11% with respect to the mean.

Finally, in Figure 3c, we show that firms that source from more districts also tend to pay higher prices for their inputs. To compute average prices, we first run a regression of log price on product fixed effects, and standardize the residual of such regression to construct our residual price index. We then normalize the average price for those firms that source from only one region to one. As shown in Figure 3c, firms that source from 5 districts pay an average price that is 0.6 standard deviations higher than firms that source from only one district. The average price paid monotonically increases with the number of districts sourced from.

Figure 3: Supplier characteristics by number of districts sourced from



(a) Distance to suppliers

(b) Average rainfall

(c) Average price of inputs

*Note.* In the left panel, we compute the average distance between the firm and each of its suppliers from our transaction data. We then compute the average distance across firm-product pairs sourcing from 1, 2,..., 5 districts. In the middle panel, for each firm-product pair, we compute the average daily rainfall at each of the districts the firm sources from. Daily rainfall comes from the India Meteorological Department. We then compute the average across all firm-product-pairs sourcing from 1, 2, ..., 5 districts. In the right panel, we compute the average price paid for inputs for firm-product pairs sourcing from 1, 2,..., 5 districts. To construct our price index, we first run a regression of log prices on product fixed effects and take the residual. We standardize the residual and normalize it to 1 for firm-product pairs that source from only one district.

## 2.3 Event-Study Analysis

We proceed by documenting how firms respond to climate-driven supply-chain disruptions. We leverage the timing of these unexpected weather shocks to examine how sales and purchases change in the lead-up to and right after the shock. Our goal is to isolate the effect of the shock from other determinants that drive changes in sales and purchases.

We set up an event-study analysis that allows us to examine pre-trends in the lead-up to the shock, and dynamics thereafter. The absence of pre-trends may provide suggestive evidence that our parallel-trends identification assumption is likely to hold, whereas the post-shock dynamics are informative of how long it takes for firms to recover after the flood.

First, we study how the shock directly affected suppliers in flood-hit regions. Then, we use the existing supplier network (in the pre-shock period) as a measure of the exposure to the shock, to study how buyers were affected when their suppliers were hit with shocks. Intuitively, we want to compare two firms that faced the same demand and productivity shocks and only differed in the location of their suppliers. By comparing the observed disruptions of a firm whose suppliers were more exposed to floods with a similar firm whose suppliers were less exposed, we can isolate the impact driven by supply-chain disruptions.

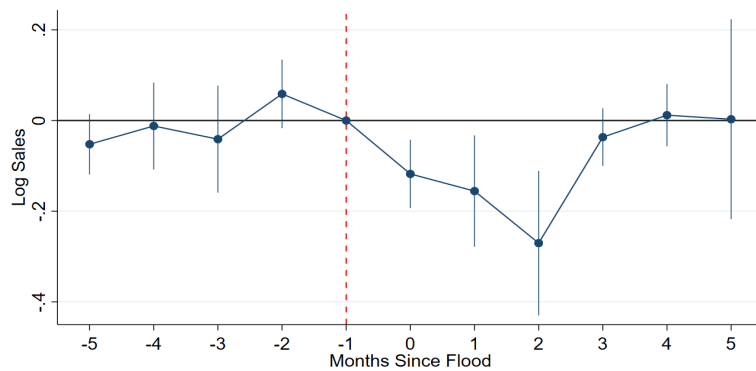
**Effects on Suppliers in Flood-hit Regions.** We begin with documenting the direct effect on suppliers in flood-hit zones with the specification, where we examine outcomes  $y_{j,t,k,\tau}$  for firm  $j$ , in period  $t$ , and industry  $k$ , measured in event-time (since flood)  $\tau$ :

$$y_{j,t,k,\tau} = \sum_{x=-5}^{x=+5} [\alpha_x \mathbb{1}(\text{Exposed to flood})_{j\tau} + \delta_{\tau,x} + \beta_x X_{j,\tau_0-1}] + \delta_j + \delta_{k,t} + \epsilon_{j,t,k,\tau} \quad (1)$$

Here, the variable ‘Exposed to flood $_{j\tau}$ ’ takes a value of 1 if firm  $j$  was exposed to a particular flood. We include a wide range of high-dimensional fixed effects to account for confounding shocks. These include firm fixed effects  $\delta_j$  that control for firm-specific time-invariant differences; industry-by-time fixed effects  $\delta_{k,t}$  that control for industry-specific shocks; and flood event-time since flood fixed effects  $\delta_{\tau,x}$  that control for aggregate trends around the flood event that affect all firms (including those not in the flood-exposed areas). We also control for firm size-specific shocks, by controlling for purchases in the pre-period  $X_{j,\tau_0-1}$ , interacted with time-since flood indicators. The sample consists of firms that had positive sales in the month before a flood.

Figure 4 plots  $\alpha_x$ , which are time dummies that capture the differential impacts on firms that were directly exposed to the flood, relative to other (non-flood-hit) firms that had positive sales in the month before a flood. The figure shows a lack of meaningful pre-trends in the lead-up to the flood. After the flood, there is an immediate decline in sales, that continues till two months after the flood. About two months after the flood, sales are about 0.25 log points lower than baseline sales. After the two-month slump in sales, there is a quick recovery, and four months after the flood, sales recover to be what they were in the pre-period.

Figure 4: Sales of Affected Suppliers



*Note.* Event-study specification documenting sales of firms that were exposed to floods in month= 0. The specification includes firm, time, event-time, and industry-real time fixed effects, and log pre-period sales-time controls. Standard errors clustered at the district level.

**Effects on Downstream Firms.** To examine how buyers are affected we need to first define a buyer’s exposure to the floods. We define a firm  $j$ ’s supplier exposure to be how exposed its suppliers were to the flood:

$$(\text{Supplier Exposure})_{j\tau} = \sum_i^N s_{i,j,\tau_0-1} \times \mathbb{1}(\text{Supplier } i \text{ exposed to flood in } \tau) ,$$

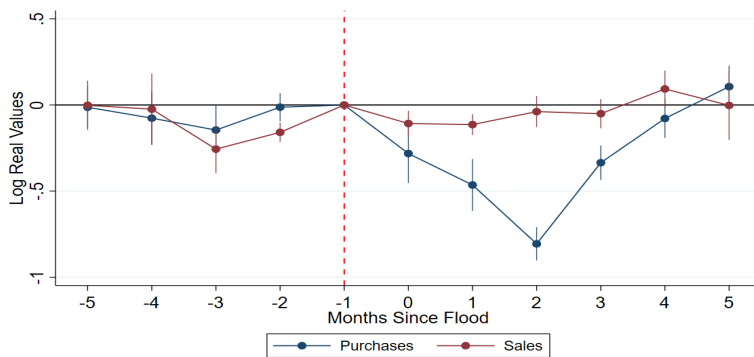
where  $s_{i,j,\tau_0-1}$  is the value of purchases that firm  $j$  buys from firm  $i$ , relative to firm  $j$ ’s total purchases, just before the flood. The index, essentially, calculates the weighted average of the flood exposure of firm  $j$ ’s sellers. A higher value of the index implies firm  $j$  faces a higher “supplier-risk,” as a larger share of its purchases were coming from firms exposed to the flood.

With the help of this variable, we can now study the outcomes  $y_{j,t,k,\tau}$  of downstream firms  $j$  in period  $t$ , industry  $k$ , and time-since flood  $\tau$ :

$$y_{j,t,k,\tau} = \sum_{x=-5}^{x=+5} [\gamma_x (\text{Supplier Exposure})_{j\tau} + \delta_{\tau,x} + \beta_x X_{j,\tau_0-1}] + \delta_j + \delta_{r,k,t} + \epsilon_{j,t,k,\tau} \quad (2)$$

Once again, we control for firm-specific time-invariant factors  $\delta_j$ ; industry-by-district-by-time fixed effects  $\delta_{k,r,t}$  that control for industry-by-region specific shocks; and flood event-time since flood fixed effects  $\delta_{\tau,x}$  that control for aggregate trends around the flood event that affect all firms.  $X_{j,\tau_0-1}$ , interacted with time-since flood indicators controls for firm size-specific shocks.

Figure 5: Purchases and Sales of Downstream Firms



*Note.* Event-study specification documenting sales and purchases of downstream firms that were exposed to floods in month= 0. The specification includes firm, time, event-time, and industry-district-real time fixed effects, and log pre-period sales-time controls. Standard errors clustered at the district level.

Figure 5 plots coefficients  $\gamma_x$ , which are time indicators that capture the differential outcomes (sales or purchases) of downstream firms with higher supplier risk. Once again, the coefficients in the pre-periods do not display any meaningful trends, suggesting that per-

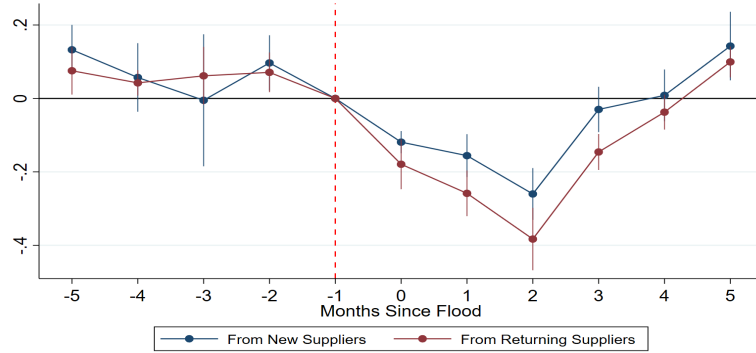
haps high and low-exposed firms had similar trends, at least in the pre-flood period.

Consistent with Figure 4, we find that purchases decline sharply for the first few months, and then start recovering. Purchases are lowest at two months after the flood, but are back to the pre-period levels by four months after the flood. This pattern follows closely with what happens to the sales for directly affected suppliers in Figure 4.

Interestingly, however, Figure 5 also shows that the sales of downstream firms are relatively modestly affected. We discuss this non-response of sales below.

**New Suppliers vs. Existing Suppliers.** Suppliers being hit by temporary shocks may induce buyers to seek out new suppliers. We compare what happens to purchases from new suppliers and existing suppliers in Figure 6, to examine this switching behavior. The blue line shows that, if anything, there is a temporary fall in purchases from new suppliers as well. There is, as expected, a meaningful fall in purchases from existing suppliers, which recovers strongly eventually. In general, buyers are unlikely to create new links, and revert back to their existing suppliers after the shock abates. These patterns are consistent with evidence from the same context that highlights how buyer-supplier relationships are personalized as relationship-capital is important ([Cevallos Fujiy et al., 2022](#)), and as a result, firms are unlikely to switch to other suppliers in the face of temporary shocks ([Cevallos Fujiy et al., 2021](#)).

Figure 6: Purchases from Existing or New Suppliers

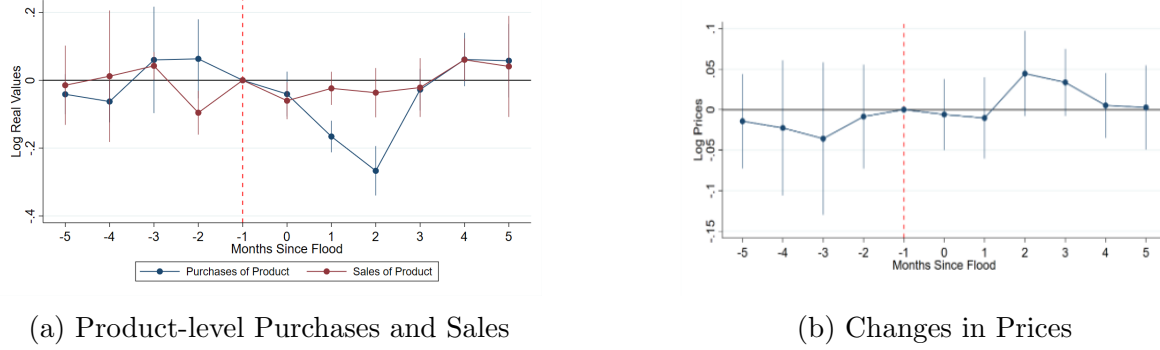


*Note.* Figures include firm, time, event-time, and industry-district-real time fixed effects, and demand controls and log pre-period purchases-time controls. Standard errors clustered at the district level.

**Products and Prices.** An advantage of our version of the firm-to-firm trade data is that it has detailed product codes and unit values. This allows us to examine product-specific trades, and changes in prices as a result of upstream suppliers being exposed to a shock. We first transform the data to be at the buyer-by-product-by-time level. Figure 7a shows the results of a higher incidence of shocks to upstream suppliers affects sales and purchases of downstream buyers. Our specification is similar to Equation 2,

but with a product dimension that allows us to include event-time, industry-district-product-time, and firm-by-product fixed effects, along with controls for pre-period firm-by-product sales interacted with time indicators. Figure 7a shows similar patterns to before, that downstream purchases fall, even as sales of downstream firms do not change substantially.

Figure 7: Product-level Trade and Prices



(a) Product-level Purchases and Sales

(b) Changes in Prices

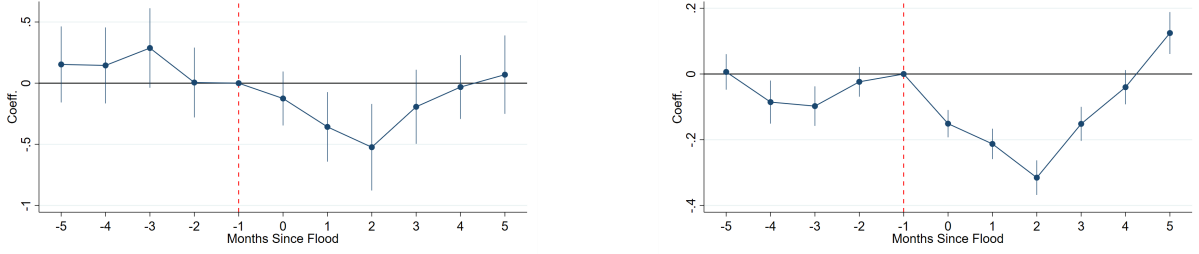
*Note.* Figure 7a includes event-time, industry-district-product-time, and firm-by-product fixed effects, along with controls for pre-period firm-by-product sales interacted with time indicators. Figure 7b includes product-time, firm-product, and event-time fixed effects. Standard errors clustered at the district level.

In Figure 7b we study the evolution of product-specific prices for transactions that occur around the flood. While noisier, there seems to be an increase in price-levels two months after the flood, but they recover, and come back to the baseline levels four months since the flood event.

**New advancements in Two-way Fixed Effects Methods.** Recent econometric advancements in two-way fixed effects methods point out that staggered treatment can lead to the negative weighting of certain disaggregated treatment effects (Goodman-Bacon, 2018). New methods developed by Borusyak et al. (2021); Callaway and Sant'Anna (2020); Sun and Abraham (2020) provide consistent and interpretable estimates. Yet, our setting offers some further challenges. Our ‘treatment’ (index) is continuous, turns ‘off’ and ‘on’ and perhaps ‘on’ again, and our specifications control for various time-varying covariates, and a wide variety of other fixed effects, making none of these new advances a suitable benchmark in our setting. A new Local Projections Difference-in-Differences (LP-DID) estimator developed by Dube et al. (2023) allows us to recover interpretable estimates in a flexible and efficient manner.

We present the results from this LP-DID estimator, which shows similar patterns. In implementing this method, we need to take a stand on using the continuous treatment variable, or a more conventional discretized one. We first study purchases for buyers in Figure 8a using the continuous treatment variable. In Figure 8b, we discretize the

Figure 8: Linear Projection DID: Purchases for Buyers



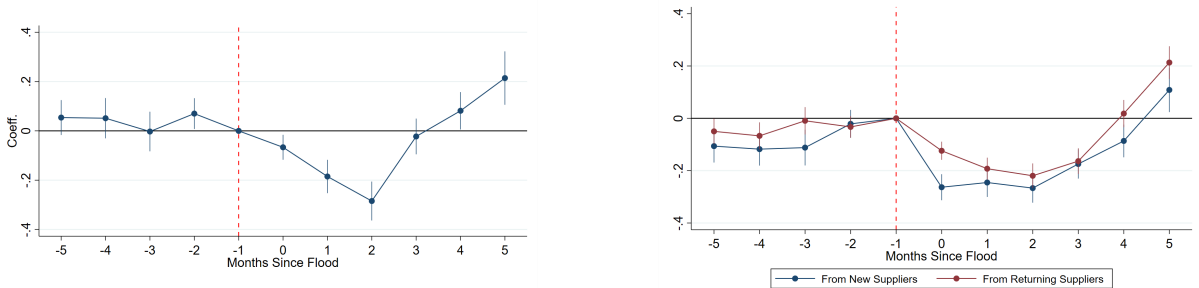
(a) LP-DID Continuous

(b) LP-DID Discrete

*Note.* Specification includes firm, flood, and industry-district-month fixed effects. Controls include log pre-period purchases interacted with time indicators. Figure 8b discretizes the treatment variable, by being equal to 1 if more than 5 percent of weighted-purchases were from affected suppliers. Standard errors clustered at the district level.

treatment variable, and once again reproduce the same pattern as before: purchases fall for the first few months, and thereafter recover by month 4.

Figure 9: Linear Projection DID: Other Outcomes



(a) Sales of Affected Suppliers

(b) Buyer Purchases from Suppliers

*Note.* Figure 9a includes firm, flood, and month-by-industry fixed effects. Figure 9b includes firm, flood, and industry-district-month fixed effects. Controls include log pre-period purchases interacted with time indicators. Figures discretizes the treatment variable, by being equal to 1 if more than 5 percent of weighted-purchases were from affected suppliers. Standard errors clustered at the district level.

The results from the LP-DID method qualitatively resemble our main results for all other outcomes as well. Figure 9a shows the sales of affected suppliers, and Figure 9b contrasts existing vs. new suppliers. These patterns once again show that sales of affected suppliers fall, and that purchases from buyers decrease from both new and existing suppliers.

### 3 Model

This section develops a spatial general equilibrium model of firm sourcing under risk, and performs comparative statics. Section 4 calibrates and quantifies the model.

### 3.1 Setting

The economy consists of  $I$  regions. Each region is endowed with  $L_i$  workers, a unit continuum of final goods producers who produce non-traded final goods, and competitive intermediate goods producers.

**Timing** A period is divided into two stages. In the first stage, final goods producers in location  $i$  place their orders for intermediate inputs from location  $j$ ,  $M_{ji}$ . In the second stage, sourcing disruption shocks are realized, and inputs are produced and delivered. Final goods firms choose their labor inputs and produce, households supply labor and consume, and all markets clear at equilibrium prices.

**Households** The household in region  $i$  supplies labor  $L_i$  inelastically to firms in  $i$  and consumes a CES aggregate of the non-traded regional final goods  $q_i$  with elasticity of substitution  $\sigma > 1$ . It solves

$$\max_{q_i(\omega)} \left( \int_{\omega \in [0,1]} q_i(\omega)^{\frac{\sigma-1}{\sigma}} d\omega \right)^{\frac{\sigma}{\sigma-1}} .$$

such that

$$\int_{\omega \in [0,1]} p_i(\omega) q_i(\omega) = w_i L_i , \quad (3)$$

where  $p_i(\omega)$  is the price of final good  $q_i(\omega)$  and  $w_i$  is the wage in region  $i$ . Our baseline model assumes labor is immobile across regions.

**Intermediate goods producers** In each region there are a continuum of competitive suppliers of tradable intermediate inputs  $M_i$  with production function  $M_i = z_i \ell_i^M$ , where  $z_i$  is their productivity. The price of intermediates in  $i$  is equal to their constant marginal cost,  $p_i^M = \frac{w_i}{z_i}$ .

Let  $p_{ji}^M$  denote the price of intermediates from  $j$  used in  $i$ . We assume iceberg trade costs  $\tau_{ji}$  between regions. No arbitrage in shipping implies that the price “at the factory gate” and the price at the time of intermediate usage are related by:  $p_{ji}^M = \tau_{ji} p_i^M$ .

**Final goods firms** Each region  $i$  contains a unit continuum of homogenous final goods producers that produce differentiated varieties  $\omega$ . Final goods are not tradable across regions. The constant returns to scale production function of the firms is

$$q_i(\omega) = \phi_i(\omega) \ell_i(\omega)^\beta x_i(\omega)^{1-\beta} , \quad (4)$$

where  $\phi_i(\omega)$  is firm productivity,  $\ell_i(\omega)$  is the firm's labor input, and intermediates  $x_i(\omega)$  can be sourced from each region  $j \in I$  as perfect substitutes.<sup>3</sup>

$$x_i(\omega) = \sum_{j \in I} x_{ji}(\omega)$$

**Second stage** In the second stage, final goods firms have already placed their orders of intermediates  $M_{ji}(\omega)$ , shocks have been realized, and production takes place. The profit maximization problem of a final goods firm in  $i$  in the second stage is

$$\max_{q, \{x_{jk}\}, \ell} [Y_i \mathbb{P}_i^{\sigma-1}]^{\frac{1}{\sigma}} q_i(\omega)^{\frac{\sigma-1}{\sigma}} - w_i \ell_i(\omega) \quad (5)$$

$$\text{such that } x_i(\omega) = \sum_{j \in I} x_{ji}(\omega) \quad (6)$$

$$x_{ji}(\omega) \leq \chi_j M_{ji}(\omega) \quad \forall j, \quad (7)$$

and the production function (4). Here,  $Y_i$  is income, and  $\mathbb{P}_i$  the price index in region  $i$ .  $\chi_j \leq 1, j \in I$  are the shock realizations. We assume the shocks destroy some of the orders of inputs  $M_{ji}$  that have been placed in the region in the first stage, and so if a shock materializes, the firm receives fewer inputs than its order. This captures the notion of climate-associated shocks such as rainfall or floods, and we will calibrate the shock size to match our event study estimates in Section 2.3. We assume the stochastic shocks are region-specific, and so they affect orders of inputs from all buying regions. As the shocks are not idiosyncratic, they will potentially affect aggregate outcomes.

Note that as second-stage profits (5) are monotonically increasing in input usage  $x_i(\omega)$ , the firm will always optimally use all available inputs that are delivered of its orders  $M_{ji}(\omega)$ . In other words, equation (7) will always hold with equality.

The first order conditions of the firm's second stage problem (5) pin down a firm's optimal choices of labor  $l_i$ , as well as its price  $p_i$ , quantity  $q_i$  and profits  $\pi_i$  as a function of orders in the first stage  $M_i = \sum M_{ji}$ . As all firms in a region are homogenous, we suppress the variety index  $\omega$  for concise exposition.

$$\pi_i(M_i) = \left[ \frac{\sigma(1-\beta) + \beta}{\beta(\sigma-1)} \right] \left[ \frac{\beta(\sigma-1)}{\sigma} \right]^{\frac{\sigma}{\beta+\sigma(1-\beta)}} w_i^{\frac{\beta(1-\sigma)}{\beta+\sigma(1-\beta)}} \left[ [Y_i \mathbb{P}_i^{\sigma-1}] \phi_i^{\sigma-1} \left( \sum_{j \in I} \chi_j M_{ji} \right)^{(1-\beta)(\sigma-1)} \right]^{\frac{1}{\beta+\sigma(1-\beta)}} \quad (8)$$

Further, the marginal contribution of increasing an order  $M_{ji}$  to second-stage profits is

---

<sup>3</sup>Alternatively, we could also use an aggregator of K varieties of inputs, where inputs of the different regions are perfect substitutes within a variety. For simplicity, our baseline model uses a single “variety” of input that can be sourced from multiple regions.

given by

$$\frac{\partial \pi(M)}{\partial M_{ji}} = \chi_j \Theta_i \left[ \sum_{j \in I} \chi_j M_{ji} \right]^{\frac{-1}{\beta + \sigma(1-\beta)}}, \quad (9)$$

where

$$\Theta_i = \left[ \frac{(1-\beta)}{\beta} \right] \left[ \frac{\beta(\sigma-1)}{\sigma} \right]^{\frac{\sigma}{\beta+\sigma(1-\beta)}} w_i^{\frac{\beta(1-\sigma)}{\beta+\sigma(1-\beta)}} [[Y_i \mathbb{P}_i^{\sigma-1}] \phi_i^{\sigma-1}]^{\frac{1}{\beta+\sigma(1-\beta)}}.$$

This implies that ex-post profits are increasing and concave in orders of inputs  $\left( \frac{(1-\beta)(\sigma-1)}{\beta+\sigma(1-\beta)} < 1 \right)$ , which will be important for the firm's stage 1 decisions below. Note that  $\Theta_i$  is stochastic as the general equilibrium regional aggregates  $Y_i$ ,  $w_i$  and  $\mathbb{P}_i$  might depend on the shock realizations across regions.

**First stage** In the first stage, prior to the realization of shocks, final goods producers in all locations choose their orders  $M_{ji}$  of inputs to maximize expected profits. As discussed above, all general equilibrium aggregates are potentially stochastic. The firm's problem in stage one is

$$\max_{M_i \geq 0} \mathbb{E}_{\chi} (\pi(M_i)) - \sum_{j \in I} p_j^i M_{ji}, \quad (10)$$

where  $p_j^i$  is the order cost of inputs from  $j$  in  $i$  and  $(\pi(M))$  is as in equation 8. The first order condition of this problem is

$$\mathbb{E}_{\chi} \left( \chi_j \Theta_i \left[ \sum_{j \in I} \chi_j M_{ji} \right]^{\frac{-1}{\beta + \sigma(1-\beta)}} \right) \leq p_j^I \quad (11)$$

### 3.2 Ex-Post General Equilibrium

In the second stage, shocks are realized, inputs are delivered across regions, and all goods and labor markets clear. The labor market clearing condition for each region  $i$  is

$$\underbrace{L_i - \frac{\bar{M}_i}{z_i}}_{\tilde{L}_i, \text{ Final goods labor}} = \left[ \frac{\beta(\sigma-1)}{\sigma} \frac{1}{w_i} [Y_i \mathbb{P}_i^{\sigma-1}]^{\frac{1}{\sigma}} \left( \phi_i \left( \sum_{j \in I} \chi_j M_{ij} \right)^{1-\beta} \right)^{\frac{\sigma-1}{\sigma}} \right]^{\frac{\sigma}{\beta+\sigma(1-\beta)}}, \quad (12)$$

where  $\tilde{L}_i$  is the labor used in the production of final goods in  $i$ , and  $\frac{\tilde{M}_i}{z_i}$  is the labor used in the production of intermediates to ship to all regions  $j \in I$  from region  $i$ .

Goods markets clear in each region implying that the region's income is equal to its expenditure

$$Y_i = w_i L_i + \hat{\Pi}_i, \quad (13)$$

where  $\hat{\Pi}_i$  aggregate profits in  $i$  are the realized profits of the final goods firms as in equation (5) less their intermediate goods order costs

$$\hat{\Pi}_i = \int \pi_i(\omega) d\omega - \int \sum_j p_{ij}^I M_{ij}(\omega) d\omega \quad (14)$$

Notice that we assume firms pay for their orders of intermediate inputs, not for the fraction they receive after the shock. Additionally, equation (12) implies that the full quantity of intermediates ordered in stage 1 is produced. This implies that the shocks 'destroy' a fraction of produced inputs.<sup>4</sup>

**Features of the equilibrium** As all firms in a region are homogenous, under the unit mass of firms assumption the regional price index  $\mathbb{P}_i = p_i$ , and aggregate profits  $\hat{\Pi}_i = \hat{\pi}_i$ . Appendix B shows that aggregate profits are a constant fraction of labor income  $\hat{\Pi}_i = \frac{1}{\sigma-1} w_i L_i$ . Further, aggregate expenditure on materials in  $i$  is given by

$$\sum_j p_{ij}^I M_{ij} = \frac{(1-\beta)(\sigma-1)}{\sigma} Y_i \quad (15)$$

These properties imply that aggregate income in location  $i$  is given by

$$Y_i = \frac{\sigma}{\sigma-1} w_i L_i, \quad (16)$$

and that the share of labor used in producing final goods in region  $i$  is constant

$$\frac{\tilde{L}_i}{L_i} = \beta \quad (17)$$

Equation (17) has strong implications for equilibrium wages. In particular, equilibrium wages need to be such that the remaining workers are allocated to the intermediate inputs sector in stage 1.

---

<sup>4</sup>We do not observe actual contracts between firms in the data, so we have to make an assumption regarding what fraction of the orders of inputs are paid for. Our setup would remain tractable under alternative assumptions, e.g. only a fraction of the order is paid for up-front. While that would change the input costs entering equation (10), it would not change the convexity of first stage profits in order costs, which is the key mechanism for firm input diversification in this framework.

In the ex-post general equilibrium, the expression for  $\Theta_i$  which is part of the marginal contribution to profits of a marginal unit of  $M_{ij}$  (equation 5) is given by the following expression

$$\Theta_i = (1 - \beta)w_i L_i \left( \sum_{j \in I} \chi_j M_{ji} \right)^{-\frac{(1-\beta)(\sigma-1)}{\beta+\sigma(1-\beta)}}.$$

This implies that  $\Theta_i$  is stochastic from the perspective of firms in stage 1.

### 3.3 A Two Location Example

To gain intuition, consider a simple case with two locations. Region 1 is risky and receives the shock with probability  $\rho$ , and region 2 is a safe location that receives no shock. Additionally, there are no trade costs, and therefore, the optimal intermediate bundle chosen by firms is the same in both locations.

We further assume that intermediates are cheaper in the risky location, that is  $p_1^I < p_2^I$ . Notice that this must hold on equilibrium, because otherwise, the safe location dominates the risky location, and the labor market will not clear in the risky location.<sup>5</sup>

The optimal stage 1 sourcing choices of firms in all regions from both regions  $i \in 1, 2$  is

$$M_{i1} : \rho \chi_1 \Theta_i^S [\chi_1 M_{i1} + M_{i2}]^{-\frac{1}{\beta+\sigma(1-\beta)}} + (1 - \rho) \Theta_i^{NS} [M_{i1} + M_{i2}]^{-\frac{1}{\beta+\sigma(1-\beta)}} = p_{i1}^I \quad (18)$$

$$M_{i2} : \rho \Theta_i^S [\chi_1 M_{i1} + M_{i2}]^{-\frac{1}{\beta+\sigma(1-\beta)}} + (1 - \rho) \Theta_i^{NS} [M_{i1} + M_{i2}]^{-\frac{1}{\beta+\sigma(1-\beta)}} = p_{i2}^I, \quad (19)$$

where  $\Theta_i^S = \frac{(1-\beta)(\sigma-1)}{\sigma} Y_i (\chi_1 M_{i1} + M_{i2})^{-\frac{1}{\beta+\sigma(1-\beta)}}$  and  $\Theta_i^{NS} = \frac{(1-\beta)(\sigma-1)}{\sigma} Y_i (M_{i1} + M_{i2})^{-\frac{1}{\beta+\sigma(1-\beta)}}$ .

As discussed above,  $\Theta_i$  is stochastic, and depends on whether or not the shock materializes in region 1. Under the monopolistic competition assumption, all firms take these aggregates as given. Plugging these shifters into the first order conditions of the firms, we can solve for optimal orders as a function of wages:

$$M_{i1} = \frac{(1 - \beta)(\sigma - 1)}{\sigma} Y_i \left[ \frac{1 - \rho}{p_{i1}^I - \chi_1 p_{i2}^I} - \frac{\rho}{p_{i2}^I - p_{i1}^I} \right] \quad (20)$$

$$M_{i2} = \frac{(1 - \beta)(\sigma - 1)}{\sigma} Y_i \left[ \frac{\rho}{p_{i2}^I - p_{i1}^I} - \frac{(1 - \rho)\chi_1}{p_{i1}^I - \chi_1 p_{i2}^I} \right] \quad (21)$$

Let wages in the less risky region 2 be the numeraire. As intermediates are priced at

---

<sup>5</sup>The fact that in this simple case, we have an interior solution for firms in both locations does not hold in general when there are multiple locations and trade costs.

marginal cost and from the labor market clearing condition (equation 12), a constant fraction of labor is used in the production of intermediates, we can show that equilibrium wages in the risky region 1 are given by

$$w_1 = \frac{z_1}{z_2} \frac{z_1 L_1 \chi_1 + z_2 L_2 (1 - \rho(1 - \chi_1))}{z_1 L_1 (\rho + \chi_1(1 - \rho)) + z_2 L_2} \quad (22)$$

### 3.4 Comparative Statics

For a larger number of regions, the model does not have an analytical solution. Prior to a full calibration to districts in India in Section 4.1, we first illustrate the model's properties in a stylized 3-region setting.

To narrow the focus to the role of varied risk across space in firm sourcing decisions, we assume the regions are homogenous in the productivity of their firms  $\phi_i$ , their labor endowment  $L_i$  and the productivity of their intermediate goods producers  $z_i$ . Trade is costly between regions and increasing in distance with elasticity 0.1. Finally, we assume that if a shock occurs, 90% of the inputs ordered are destroyed ( $\chi = 0.1$ ).

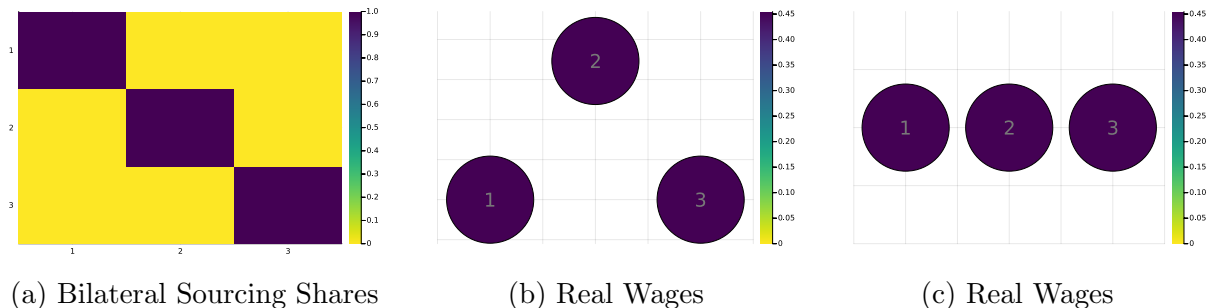
We consider two situations. First, we look into the case where the three locations are equidistant from each other. Second, we allow for regions to also vary in their distance to each other. The results for the first scenario highlight how firms diversify their suppliers without the feature that some suppliers are closer than others. The second adds geography as an additional margin that affects input sourcing choices. For stark comparative statics, we place the three regions on a straight line. This allows for a possible tradeoff between the diversification motive and higher trade costs of sourcing from further regions. In some experiments, we also vary the probabilities of shocks across regions.

We consider five experiments. In the first, “no risk” experiment, we assume  $\rho_i = 0$  for all regions. In the second, “homogenous risk” case, we assume a constant shock probability across space. That is, we assume  $\rho_i = 0.15$  for all  $i$ . In the third, “heterogeneous risk” scenario, we assume the shock probability varies across space, with the average shock probability the same as the homogeneous risk case ( $\frac{1}{I} \sum_{i=1}^3 \rho_i = 0.15$ ). In the fourth, “heterogeneous risk in autarky” case, we raise trade costs to infinity, effectively prohibiting inter-regional input sourcing. In the fifth, “heterogeneous risk with free trade” case, we set trade costs to 0 across regions. The probabilities of shocks in cases four and five are the same as in the baseline heterogeneous risk case 3.

**Case 1: No Risk.** Figure 10 illustrates the sourcing shares and expected real wages when  $\rho = 0$  for all regions. With identical fundamentals and positive trade costs, it is optimal for every firm to source all inputs domestically within its own region. This is true

regardless of geography. Figure 10a illustrates the diagonal terms are 1, i.e., within-region sourcing shares are 1 for all regions, and cross-region sourcing shares are zero. The figure also makes clear that expected real wages are equalized across all regions under both geographies. This setting benchmarks our model relative to typical trade and spatial models where there is no sourcing risk. As all regions are identical, there are no gains from trade and the equilibrium is regional autarky. In particular, the contrast between equidistant regions and regions on a line does not change either sourcing shares or regional real wages. There is no role for geography in the equilibrium with no risk and positive trade costs.

Figure 10: Scenario with no risk

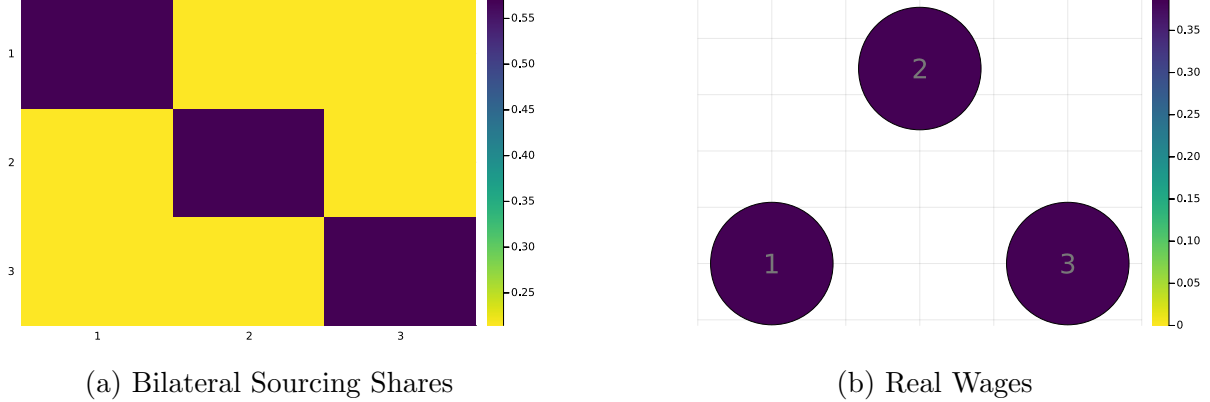


*Note.* Panel A shows the  $3 \times 3$  input-output matrix where the buying regions are in the vertical axis and the supplying regions are in the horizontal axis. Each row represents the share of inputs purchased by a buying region from each (column) supplying region. In the scenario with no risk, the sourcing shares in Panel A are the sourcing shares for the geographies in Panels B and C. Panels B and C present the real wages for each region, as well as a visual representation of the geographical location of regions in space. In Panel B, regions are equidistant from each other. In Panel C, regions are in a straight line, implying that the regions have different distances from each other.

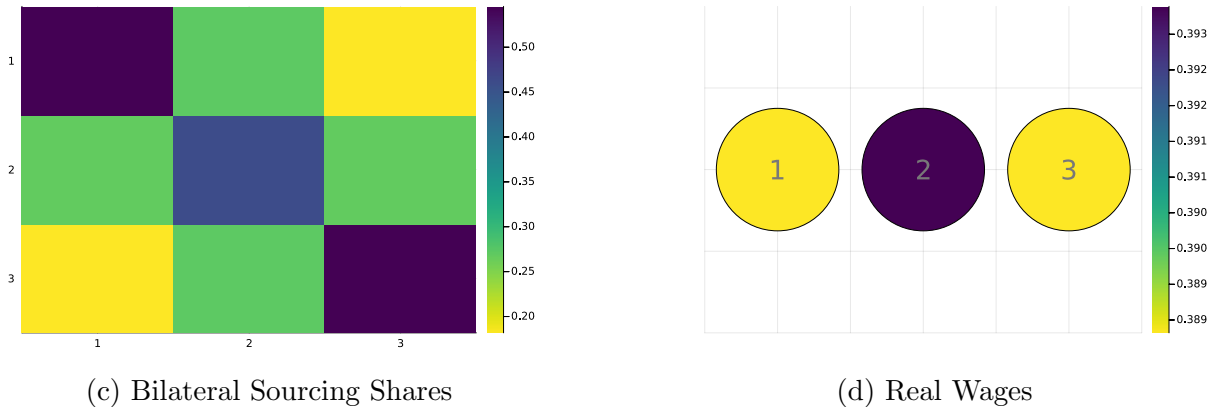
**Case 2: Homogeneous Risk.** Figure 11 illustrates the bilateral sourcing shares when the risk of shocks in each region is  $\rho = 0.15$ . Firms now face a tradeoff: as shocks are independent across regions, they can reduce the probability of input disruptions by sourcing from multiple regions. On the other hand, sourcing from other regions is costly, due to the trade costs. As a result, firms still largely source inputs from their own regions, but also diversify by sourcing some inputs from geographically closer regions where trade costs are lower. Panel B illustrates that this higher demand for inputs from more central regions in equilibrium results in higher expected real wages in these regions. These more central regions also diversify their risk the most by participating in interregional sourcing. Note that the expected price index in more central regions is therefore lower in equilibrium, as firms from these regions pay less in trade costs for inputs and better diversify risk. In contrast, Panel A shows that while firms diversify risk with some interregional sourcing, there is no geographic variation in expected real wages or in sourcing patterns with equidistant regions.

Figure 11: Scenario with homogeneous risk

Panel A: Same distance between regions



Panel B: Different distance between regions



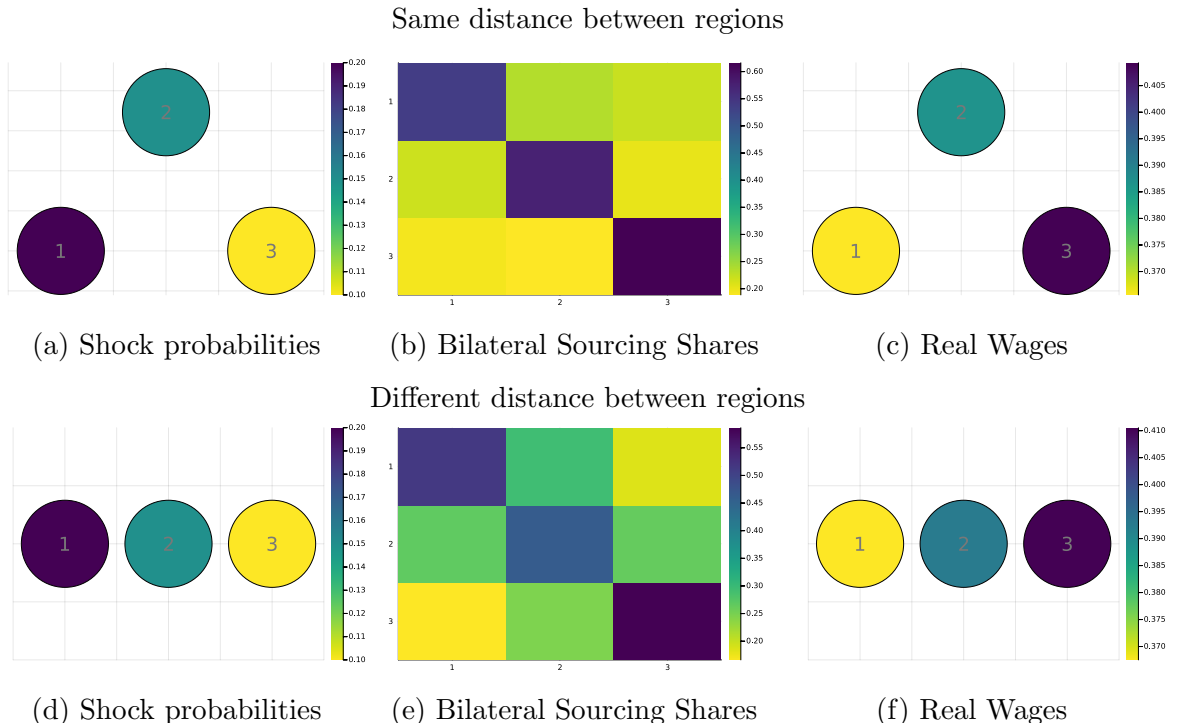
*Note.* The figures in the left panel consist of a 3x3 input-output matrix where the buying regions are in the vertical axis and the supplying regions are in the horizontal axis. Each line represents the share of inputs purchased by a buying region from each supplying region (column). The figures in the right panels present the real wages for each region, as well as a visual representation of the geographical location of regions in space. In Panel A, regions are equidistant from each other. In Panel B, regions are in a straight line, such that the regions have different distances between each other. The scales are shown to the left of each figure.

**Case 3: Heterogeneous Risk.** The left panels of Figure 14a illustrates the regional maps and the shock probabilities of each region in the heterogeneous risk case under both equidistant regions and heterogeneous distance. The middle panels show the bilateral sourcing shares between regions. The diagonal is again the darkest, in the presence of trade costs all regions source most of their inputs from their own region despite heterogeneous risk. However, there is clear variation. Region 1, the riskiest region, has the smallest “own sourcing” share in both geographies while the safest region 3 sees the most “own sourcing”. All regions source inputs from other regions, with relatively larger shares from those with low risk. Geography plays an important role too. In the top panel, with equidistant regions, the riskiest region 1 has a high sourcing share from the safest region

3. With regions on a line in the bottom panel, however, region 1 is now further from the safe region, and so its sourcing share from region 3 decreases.

The right panels show that expected real wages across regions are negatively correlated with the risk of shocks, and are highest in safest locations despite identical regional fundamentals. The underlying mechanisms at work are that safer regions experience higher labor demand for their intermediate inputs from all regions, pushing up nominal wages. They also face a lower price index of their final goods, as they can source safer “domestic” inputs without paying trade costs. Notice that in general equilibrium, the wage impacts on safer regions will modulate sourcing from them. As a result, even with equidistant regions, the safe region does not see the highest sourcing shares from all other regions.

Figure 12: Scenario with heterogeneous risk



*Note.* The figures in the left panel show the probability that each region is hit by a shock, as well as a visual representation of the geographical location of regions in space. The figures in the middle panel consist of a 3x3 input-output matrix where the buying regions are in the vertical axis and the supplying regions are in the horizontal axis. Each line represents the share of inputs purchased by a buying regions from each supplying region. The right panels present the real wages for each region. For the top panels, regions are equidistant from each other. In the bottom panels, regions are in a straight line, such that the regions have different distances between each other. The scales are shown to the left of each figure.

Importantly, under our assumption that inputs are perfect substitutes and that regions have identical fundamentals, there is no source of traditional gains from trade either through comparative advantage or increasing varieties. The incentives for trade here arise entirely to mitigate risk, with strong spatial general equilibrium implications for

wages and prices. We will return to this point below, when evaluating the welfare gains from supplier diversification.

**Comparison between homogeneous and heterogeneous risk cases.** Figure 13c compares the expected real wages and their variance between the homogeneous and heterogeneous risk cases. The left panels show the ratio of expected real wages, and the right panels show the ratio of their variance. As is immediately clear, the riskiest region 1 sees the largest declines in its expected real wages as we move from homogeneous to heterogeneous risk under both geographies, while the safest region 3 see lower expected real wages under homogenous risk. Region 2, which has the same risk under both homogenous and heterogeneous risk, sees relatively higher expected real wages when risk is heterogeneous *and* it is a central region (bottom panel). In this instance, while it is not the safest region, it is still attractive as a sourcing destination due to its central location. When it is equidistant from all regions (top panel), its expected real wages are similar between trade and autarky. The right panels of the figure show that all regions see a decline in the variance of their expected real wages in the heterogeneous risk case relative to homogeneous risk. The safest region 3 sees some of the largest declines, as its shock probability decreases moving to heterogeneous risk. However, the decline in expected wage variance for region 3 is larger when it is equidistant from all regions and can diversify its risk at lower cost, than when it is further away (bottom panel). The riskiest region 1 also sees a larger decline in its wage variance when it is equidistant from all regions and can diversify its higher risk at lower cost, than when it is further away from the safest region 3 (bottom panel). On the other hand, Region 2 sees a larger decline in wage variance when regional distance is heterogeneous, as it benefits from its central location and better ability to diversify risk at lower cost in this instance.

**Case 4: Heterogeneous Risk and Autarky.** We next maintain the heterogeneous risk across regions but raise trade costs to infinity, shutting down inter-regional input sourcing. Figure 14 illustrates that while the probabilities of shocks remain the same as Case 3 above (left panel), bilateral sourcing mimics the no-risk Case 1 (middle panel). The impact on expected real wages is very different in both Case 1 and Case 3, however (right panel). The riskiest region sees the lowest expected real wages, while the safest regions see the highest expected real wages, as they have the lowest expected prices due to the lowest shock probabilities and fully domestic sourcing. The range of expected real wages is larger in this case than with costly trade, illustrating the diversification benefit of trade in mitigating expected real wage inequality across regions in an environment with risk. In Appendix B, we show that the expected real wage patterns are similar for equidistant regions, as with autarky, regional geography has no impact on regional outcomes.

Figure 13: Comparison between homogeneous and heterogeneous risk cases

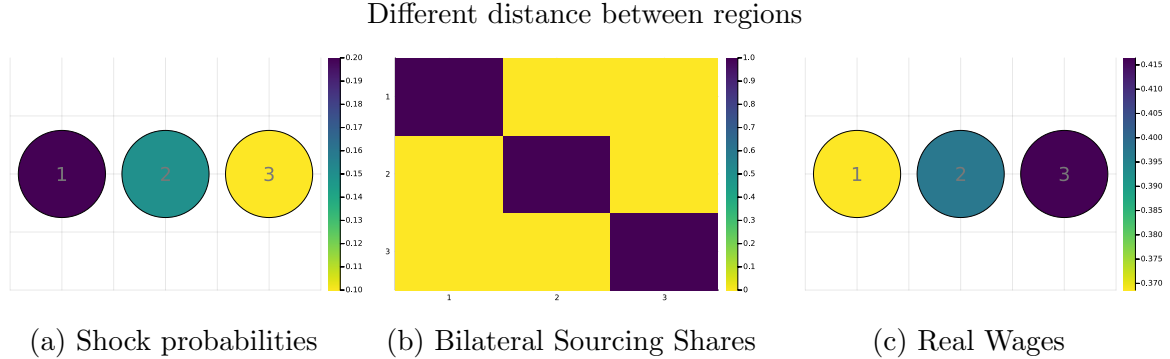


*Note.* In this figure we plot the expected real wages (left panel) and variance of real wages (right panel) for the homogeneous case shown in Figure 11 relative to the heterogeneous case shown in Figure 12. The variance of real wages is computed across potential states of the world. For the top panels, regions are equidistant from each other. In the bottom panels, regions are in a straight line, such that the regions have different distances between each other. The scales are shown to the left of each figure.

**Welfare Comparison between Costly Trade and Autarky with Heterogeneous Risk Cases.** We next consider how expected real wages change across regions moving from costly trade to autarky in Panel A, Figure 15. Interestingly, all regions see a decline in expected real wages moving to trade from autarky. The intuition is that in this setting, there are no “conventional” gains from trade, as there is no comparative advantage or gains from variety. The primary reason for trade here is for risk diversification. However, trade is costly, so the benefits of diversification are obtained at a higher average input price, raising regional price indices and lowering expected real wages under costly trade. The smallest decline in real wages is for the riskiest region 1, which is due to its expected real wages being relatively low in autarky as well as its high shock probability.

While the diversification motive for trade does not improve welfare as measured by the

Figure 14: Scenario with heterogeneous risk and infinite trade costs



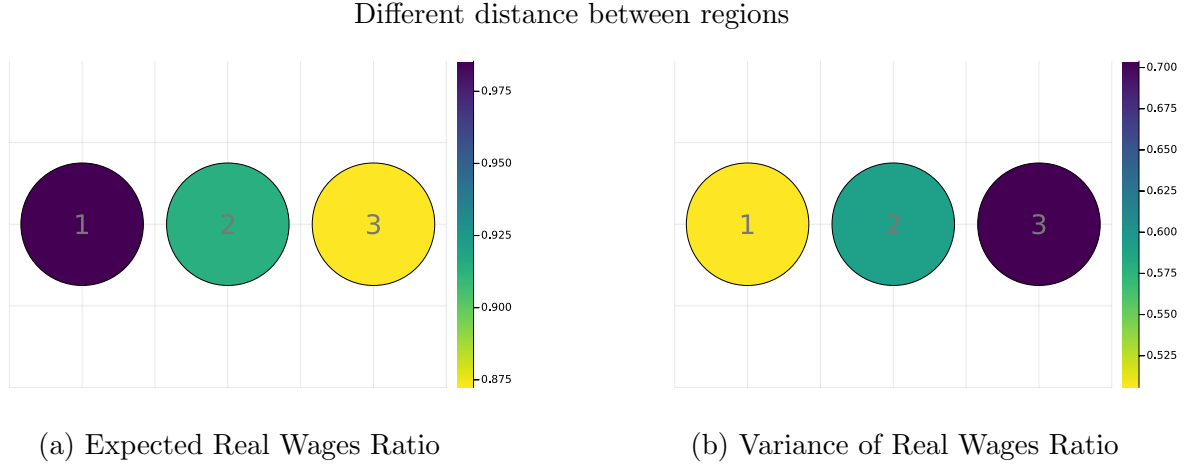
*Note.* This figure presents the case where trade costs are set to infinity. The figures in the left panel show the probability that each region is hit by a shock, as well as a visual representation of the geographical location of regions in space. The figures in the middle panel consist of a 3x3 input-output matrix where the buying regions are in the vertical axis and the supplying regions are in the horizontal axis. Each line represents the share of inputs purchased by a buying regions from each supplying region. The right panel presents the expected real wages for each region. The scales are shown to the left of each figure. In this scenario, regions vary in their distance and are located on a line. The case with equidistant regions is shown in Figure A2.

expected real wage, Panel B of the figure illustrates that the variance in real wages increases sharply, moving to costly trade from autarky for all regions. Supply chain diversification lowers the variance in final goods prices across all regions, insuring against shocks and real wage volatility. Again, the riskiest region 1 sees the largest increase in the variance of expected real wages when trade is barred. Appendix Figure A3 shows the same insight holds with equidistant regions, as regional geography primarily modulates sourcing patterns when trade is possible, but does not otherwise play a large role in the mechanisms underlying the relative decline in real wages and increase in their variance moving from costly trade to autarky.

**Case 5: Heterogeneous Risk and Free Trade.** Under free trade, firms can diversify their input risk at lower costs – the tradeoff is only that inputs in lower-risk regions will be more costly in equilibrium as those regions will see higher expected real wages. With the same fundamentals across regions and free trade, in equilibrium, every firm in every region has the same optimal sourcing strategy. The middle panel of Figure 16 illustrates these sourcing shares. The left panel illustrates that in this setting, there is increased expected real wage dispersion relative to costly trade, as sourcing concentrates in the safest location region 3, pushing up real wages there. Under free trade, regional geography plays no role in these patterns, and sourcing shares and expected real wages are the same as in this case when regions are equidistant (Figure A4).

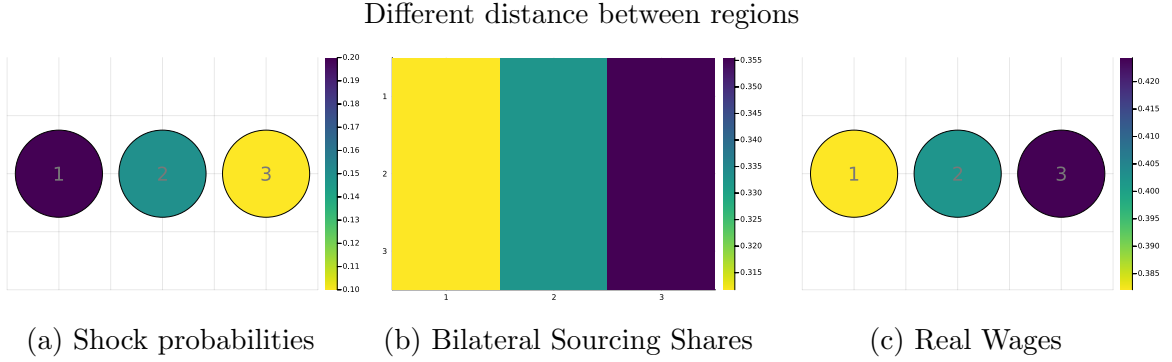
**Welfare Comparison Between Costly and Free Trade with Heterogeneous Risk.** Panel A of Figure 17 illustrates that in contrast to costly trade, all regions see higher

Figure 15: Comparison between heterogeneous risk under costly trade and autarky



*Note.* In this figure we plot the expected real wages (left panel) and variance of real wages (right panel) for the scenario with heterogeneous risk and costly trade shown in Figure 12 relative to the scenario with heterogeneous risk and trade autarky shown in Figure 14. The variance of real wages is computed across potential states of the world. Here, regions are in a straight line, such that the regions have different distances between each other. The scales are shown to the left of each figure. The case with equidistant regions is shown in Figure A3.

Figure 16: Scenario with heterogeneous risk and free trade

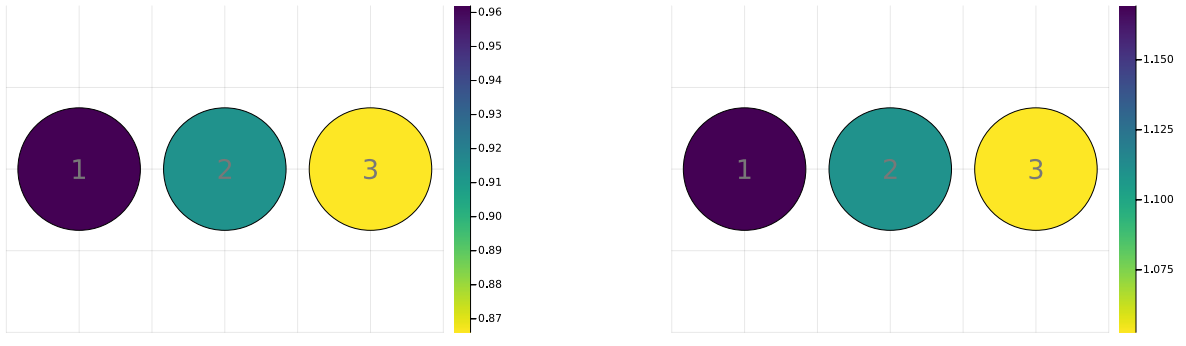


*Note.* This figure presents the case where there are no trade costs. The figure in the left panel show the probability that each region is hit by a shock, as well as a visual representation of the geographical location of regions in space. The figure in the middle panel consist of a 3x3 input-output matrix where the buying regions are in the vertical axis and the supplying regions are in the horizontal axis. Each line represents the share of inputs purchased by a buying regions from each supplying region. The right panes present the real wages for each region. The scales are shown to the left of each figure. Figure A4 illustrates the case when regions are equidistant from each other.

expected real wages under free trade. This is due to the lower costs of inputs, both from risk diversification and the lack of trade costs. The largest increases in expected real wages moving from costly to free trade are in the safer but geographically-distant region 3. This region sees increases in sourcing from all regions as firms no longer face high trade costs to access the region's lower risk inputs, but also see larger declines in its own price index as its firms do not pay large trade costs to diversify their own risk. Panel B illustrates that moving from costly to free trade also lowers the variance of expected real wages across all

regions. Thus, under free trade, there is no tradeoff between higher expected real wages and lower volatility. Similar insights hold when regions are equidistant (Figure A5).

Figure 17: Comparison between costly and free trade



(a) Expected Real Wages Ratio

(b) Variance of Real Wages Ratio

*Note.* In this figure we plot the expected real wages (left panel) and variance of real wages (right panel) for the scenario with heterogeneous risk and costly trade shown in Figure 12 relative to the scenario with heterogeneous risk and free trade shown in Figure 16. The variance of real wages is computed across potential states of the world. Here, regions are in a straight line, such that the regions have different distances between each other. The case with equidistant regions is in Figure A5. The scales are shown to the left of each figure.

## 4 Quantification

### 4.1 Calibration

We calibrate our model to 271 Indian districts, which is the finest geographical detail possible to compute the key moments needed. To calibrate the model for India as a whole, we complement our transaction data with the Annual Survey of Industries (ASI), which is a nationally representative survey of manufacturing plants in India with more than 10 employees. We primarily use the wave of 2006-07 since it is the latest year for which the ASI has publicly available data at the district level.<sup>6</sup>

We need to calibrate the following parameters and moments: the demand elasticity ( $\sigma$ ), the input disruption due to the shock ( $\chi_j$ ), labor endowments by district ( $L_i$ ), regional productivities ( $\phi_i$ ), the labor share in the production function ( $\beta$ ), iceberg trade costs ( $\tau_{ij}$ ), and flood probabilities ( $\rho_i$ ).

First, we set the demand elasticity  $\sigma$  to 2 following Boehm et al. (2020) and choose the input disruption parameter  $\chi_j$  to match a drop of 75% in buyer purchases as estimated

---

<sup>6</sup>While there are more than 500 districts in India, several of them have very low manufacturing employment in the ASI. Estimates using these districts are therefore very noisy. We aggregate districts with fewer than 10000 manufacturing workers to a single district within a state where possible, or merge them to neighboring larger districts in their own state. We present results with all districts in Appendix C.

in our event study in Figure 5. Second, we use the ASI to obtain total employment by district, which we use as labor endowments  $L_i$ .

To estimate productivities by district,  $\phi_i$ , and the labor share  $\beta$  we follow the literature on production function estimation and use the Ackerberg, Caves, and Frazer (2015) approach (henceforth ACF). This approach requires lagged values of labor and materials as instruments, and we need a panel of firms. However, the public version of the ASI is a cross-section of plants which prevents constructing a firm-level panel. As a solution, we use the waves for 2004-05, 2005-06, and 2006-7 to construct a synthetic panel at the district-industry level. We then treat each industry-district pair as a “firm” for the purposes of estimation.

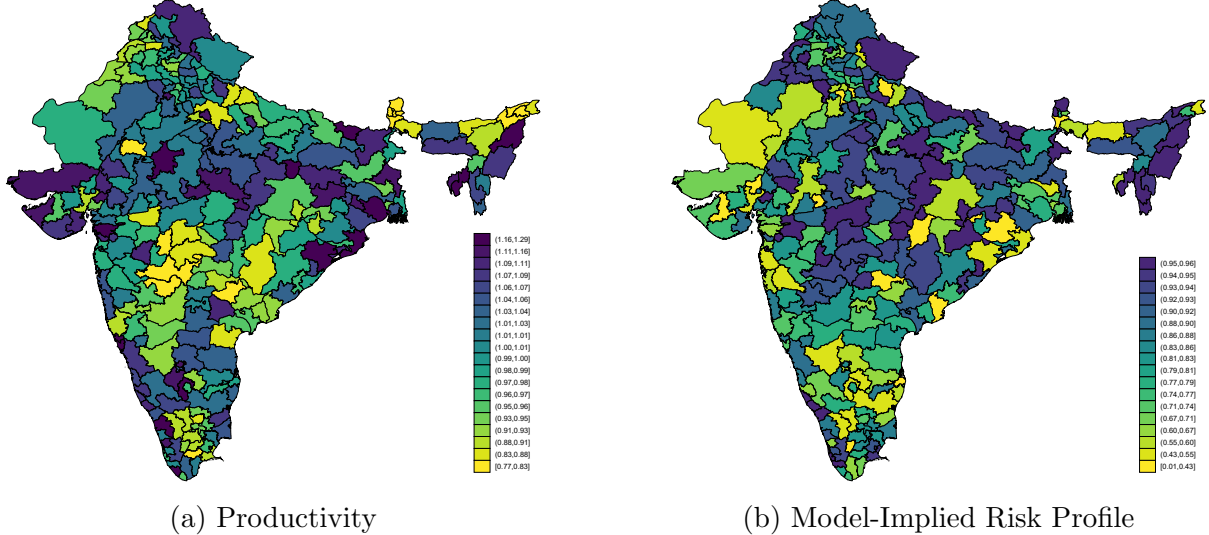
We implement the ACF procedure to estimate the production function parameters and the productivities. We use revenues as the dependent variable and labor, materials and capital as the production function inputs. The estimation process yields coherent estimates for the inputs that add up to less than one as expected. Once we back out the ACF productivity for each industry-district pair, we aggregate at the district level by using weights based on the relative importance of each industry in each district. In the few cases where productivity cannot be estimated due to missing data for smaller districts, we assign those regions the average productivity of their closest neighbors. Panel A of Figure 18 illustrates the estimated variation in district-level productivities. From the ACF procedure we also get the corresponding coefficients for labor, materials and capital. The results are shown in the left panel of Table 2, where the materials share is 0.81, the labor share 0.08 and the capital share 0.17. We compute the labor share as  $\beta = 1 - 0.81 = 0.19$ . Since we do not have capital in the model, we think of the labor share as the share of capital-augmented labor, so we include both capital and wage expenses into the calculations.

The iceberg trade costs  $\tau_{ij}$  are estimated using our transaction data. A key limitation is that our data is only available for one state, while we need to back out trade costs for each bilateral pair of districts throughout India. To deal with this, we proceed in two steps. As a first step, we use our transaction data, focus on firms in our state that sell their goods, and aggregate the data at the seller-buyer-time level. We then run a regression as in equation 23.

$$\log(p_{s,b,t,q}) = \gamma_1 \log(\text{distance from } s \text{ to } b) + \gamma_2 \mathbb{1}(b \text{ in same state as } s) + \gamma_{s,q,t} + \epsilon_{s,b,t,q} \quad (23)$$

where  $p_{s,b,t,q}$  is the price charged by seller  $s$  to buyer  $b$  for product  $q$  at time  $t$ . For each buyer-supplier pair we compute the log distance between them as reported in our trans-

Figure 18: Estimated Productivities and Risk Probabilities



*Note.* In this figure we plot the estimated district-level productivities (left panel) and the model-implied district-level shock probabilities (right panel). Productivities are estimated using the ACF procedure as described in the text. Shock probabilities are obtained by matching model-implied sourcing shares to the data as described in the text. The scales are shown to the right of each figure.

action data. We also include a dummy variable on whether the buyer ( $b$ ) is in our state. The coefficient on distance captures how prices charged change as distance increases. Importantly, we add seller-product-time fixed effects, so effectively, the coefficients  $\gamma_1$  and  $\gamma_2$  are being identified by sellers that sell the same product to multiple buyers in a given time period. Since we are doing this within seller-product-time, the estimates are not driven by firm-level shocks such as productivity that might also affect prices. The results of this regression can be found in the right panel of Table 2.

As a second step, we use the estimated coefficient to predict trade costs for the rest of India. We compute the bilateral distances between the centroid of each district and use those distances to predict trade costs between regions using the estimated coefficients  $\hat{\gamma}_1$  and  $\hat{\gamma}_2$ . We assume that the border effect estimated through coefficient  $\hat{\gamma}_2$  is the same for all states in India.

**Shock probabilities.** Our model implies that bilateral sourcing shares are pinned down by district fundamentals like productivities and labor force, and bilateral trade costs, in addition to the vector of district-level shock probabilities. Therefore, we can obtain the vector of shock probabilities  $\rho_i$  by minimizing the distance between the observed sourcing shares in the data with those implied by the model. The intuition of the exercise is as follows: conditional on the rest of the parameters and moments of the model, we pick the shock probabilities of each district to match exactly the observed share of purchases from every district in our state to each other district in India. The underlying assumption is

Table 2: Estimation Results

Panel A: Production Function Estimation		Panel B: Trade Costs Estimation	
	log(Sales)		log(Price <sub>s,b,t,q</sub> )
log(Materials)	0.81*** (0.076)	log(distance from $s$ to $b$ )	0.0174*** (0.0001)
log(Workers)	0.17*** (0.061)	$\mathbb{1}(b \text{ in same state as } s)$	-0.086*** (0.0001)
log(Fixed Capital)	0.08 (0.063)		
Number of Observations	9128	Number of Observations	65,477,898

Note. Panel A presents the results of the production function estimation using the ACF procedure. The reported coefficients are for log materials, log number of workers and log fixed capital as calculated from the ASI. Panel B presents the results for the trade costs estimation using our transaction data. The outcome is the log price charged by a seller in our state ( $s$ ), for a given product ( $q$ ), to a buyer ( $b$ ) in a given month-year period ( $t$ ). The main regressors are log distance from buyer to seller and a dummy that takes the value of 1 if the buyer is in the same state as the seller. We control for seller-product-time fixed effects.

that anything that is not captured by the district-level productivities and trade costs is part of the risk of the district. Of course, in practice, such residual does not only include flooding risk but many other risk components. However, in Figure 19a, we show that our estimated probabilities are significantly correlated with observables related to flood risk, such as average rainfall. In Figure 19b, we also show that our estimated probabilities are negatively correlated with the average night-lights luminosity index. This is consistent with higher economic activity being concentrated in lower risk areas. Importantly, in Figure A6, we show that these probabilities are not correlated with either productivities, nor the average distance to the state of our study.

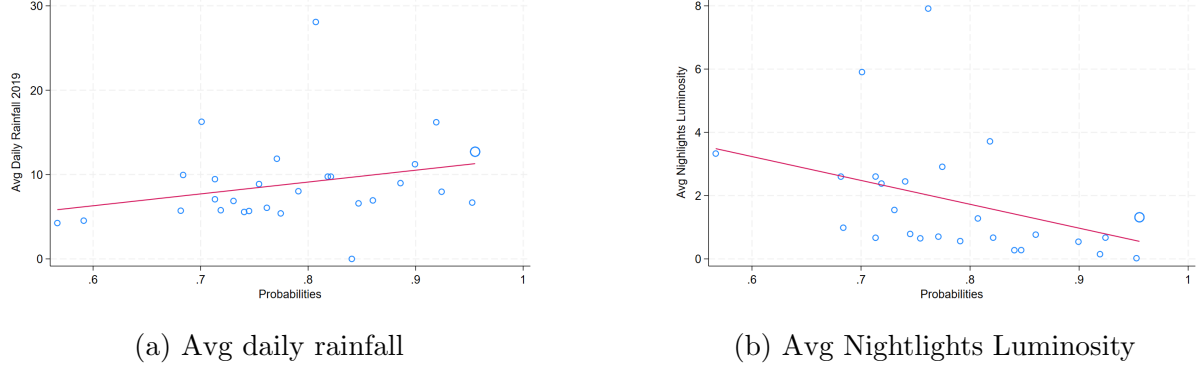
Notice that this exercise requires solving jointly for the vector of district-level risk that minimizes the gap between model implied sourcing shares and data, as all bilateral sourcing shares are equilibrium objects that depend on the fundamentals and risk of all other districts. Further, we cannot exactly match all bilateral sourcing shares in the data, as we choose a single shock probability for each district, but we observe multiple sourcing shares for that district from all districts in our “state.” We therefore set up a Miminum Distance Estimator, which aims to match the average sourcing shares for each origin district observed across all destination districts in our data. In practice, we match all the bilateral sourcing shares in the data well, as Figure 20 shows. As external validation, the right panel of Figure 20 shows that our model also matches the data on sales shares well, which are untargeted moments.<sup>7</sup>

Table 3 summarizes our model calibration.

---

<sup>7</sup>Figure A8 zooms in on low sourcing shares where much of the sample lies.

Figure 19: Model probabilities and observables



*Note.* In this figure, we plot the estimated probabilities against some observables at the state level. In Figure 19a, we correlate the probabilities with the average daily rainfall in 2019. In Figure 19b, we correlate the probabilities with a measure of average nighttime luminosity that captures economic activity as well as energy use.

Table 3: Calibrated moments

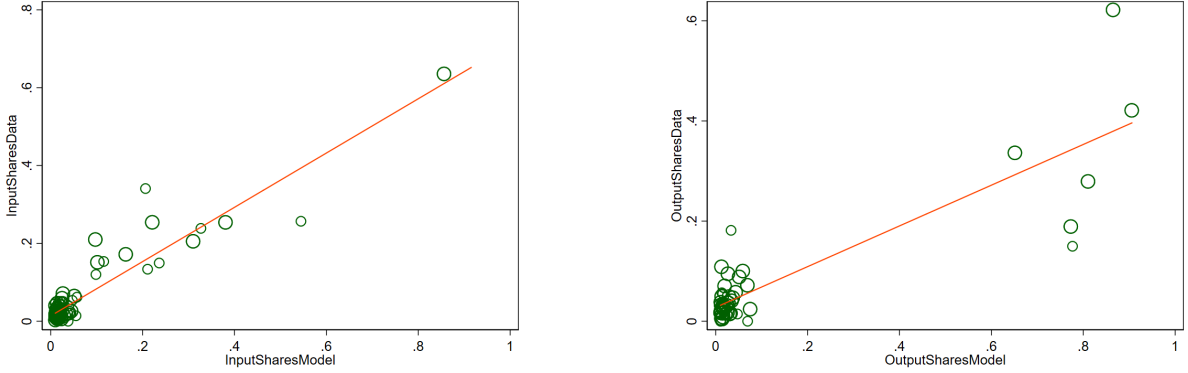
Parameter	Source
$L_i$ : Labor endowments	Annual Survey of Industries (ASI), 2019-20
$\phi_i$ : Region productivities	Ackerberg et al. (2015) estimation (ASI, 2017-2019)
$\tau_{ij}$ : Iceberg Trade costs	Regression of within firm-product price on distance between buyer and seller (Transaction data)
$\rho_i$ : Flood probabilities	Model inversion using sourcing shares across districts (Transaction data)
$\chi_i$ : Flood shock	Match drop of 75% in buyer purchases from event study (Transaction data)
$\beta$ : Labor share	0.17: Expenditure in labor and capital to total sales (ASI, 2017-2019)
$\sigma$ : Demand elasticity	2: Based on Boehm et al. (2023)

## 4.2 Quantitative Results

We begin by showing that the model delivers a strong negative relationship between shock probabilities and relative nominal wages (and real wages) in the cross-section. Figure 21 shows that both nominal and real wages are negatively correlated with shock probabilities, as we would expect. In Figure A7, we also show that the price index and the variance in real wages are negatively correlated with the shock probabilities.

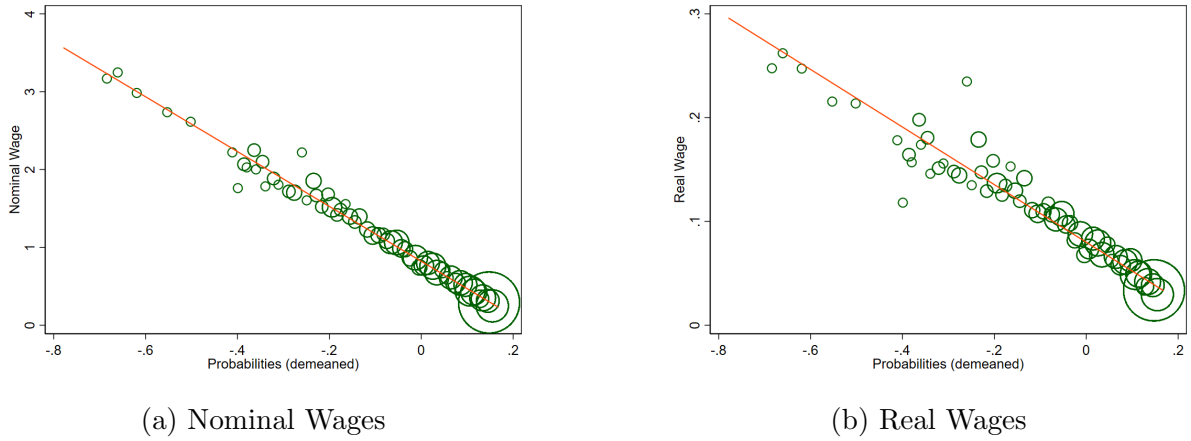
**Probabilities and Sourcing Shares** To illustrate the rich heterogeneity in bilateral sourcing patterns in the quantitative model, we show the sourcing choices of two districts

Figure 20: Sourcing Shares: Model vs. Data



*Note.* In this figure, we plot the sourcing shares in the data against the model. In the left panel we plot the input sourcing shares. We target average sourcing probabilities from our state's districts to the rest of the districts, but not forcing anything to match the particular sourcing shares of each district. In contrast, the left panel shows the input shares from each district. The right panel shows sales shares, which are entirely untargeted. Figure A8 zooms in on low sourcing shares where much of the sample lies.

Figure 21: Shock probabilities and Wages

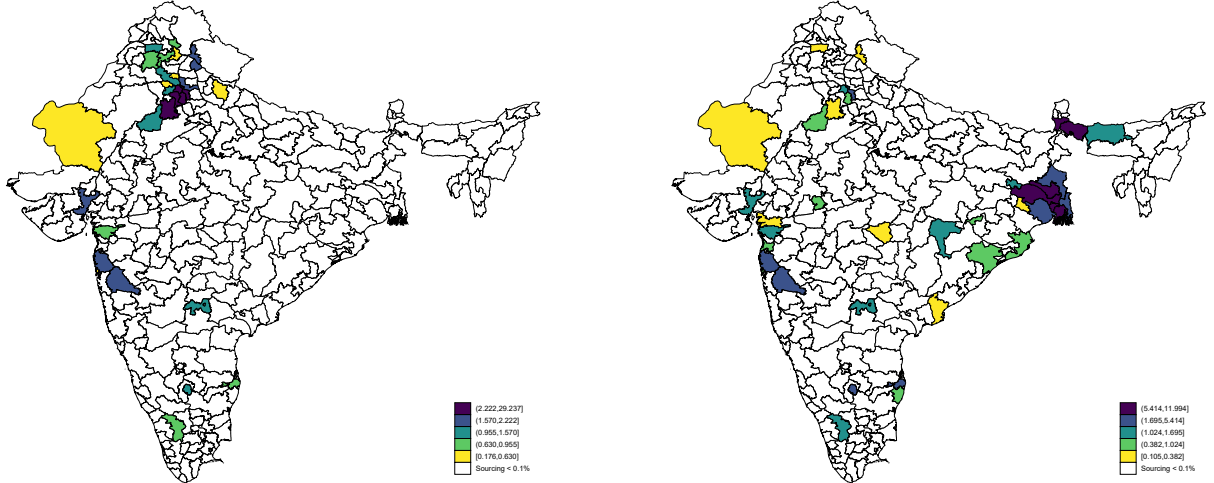


*Note.* In this figure, we plot model-derived nominal (left panel) and real (right panel) wages against the estimated shock probabilities. Figure A7 further plots the price index, and the variance in real wages against the shock probabilities.

in Figure 22. The left panel illustrates the sourcing patterns of New Delhi, a relatively low risk district. While firms still diversify, they source more from geographically closer areas. The right panel shows the sourcing shares chosen by Kolkata, a high risk district. In this case, the model implies the district's firms choose more inter-district sourcing to mitigate risk. Again geography matters, and sourcing shares are higher for closer districts. In Appendix C we show that under free trade, the sourcing patterns for all regions are identical and each region sources from districts all over the country.

**Expected real wages under baseline and autarky** The comparative statics in section 3 showed that with identical regional fundamentals, expected real wages were lower for all regions with costly trade than in autarky. To assess whether this mechanism is

Figure 22: Shock Probabilities, Delhi Sourcing, Kolkata Sourcing



quantitatively relevant in the calibrated model with varying regional fundamentals and estimated trade costs, we compute the difference in expected real wages in the baseline model with the model-implied expected real wages given the same regional fundamentals and infinite trade costs.

Figure 23 illustrates the spatial variation in expected real wages in the baseline model and in the autarky counterfactual. On average, expected real wages are 11.6% higher in the baseline model than in autarky. 5% of districts have lower expected real wages, however. The variance of real wages is 86% lower in the baseline model than in autarky, validating the quantitative relevance of the main comparative statics exercises.

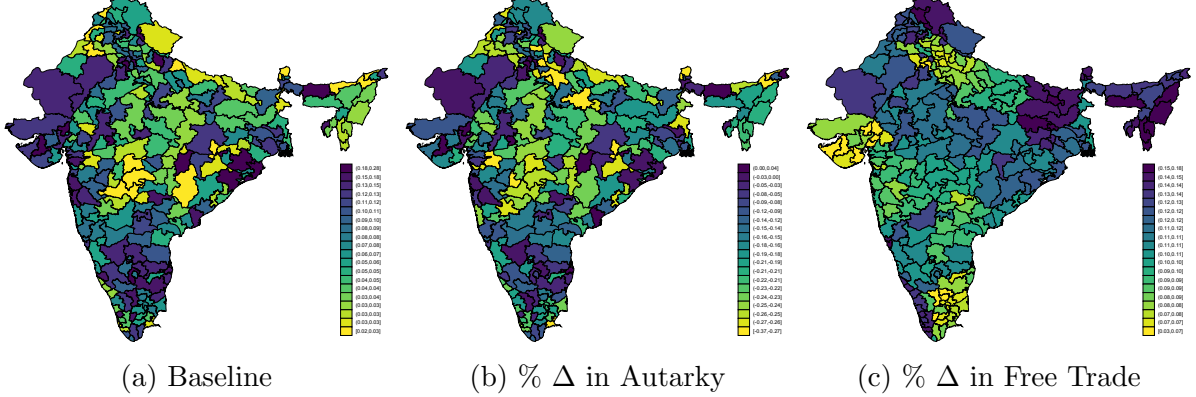
**Expected real wages under baseline and free trade** In contrast, Figure 23 shows that expected real wages are higher for many regions under a free trade counterfactual. To implement free trade in our quantitative exercise, we set the iceberg trade costs to 1 between all districts. Under free trade, expected real wages are on average 13.4% higher than in the baseline, whereas the variance of real wages is 24.5% lower.

## 5 Counterfactuals

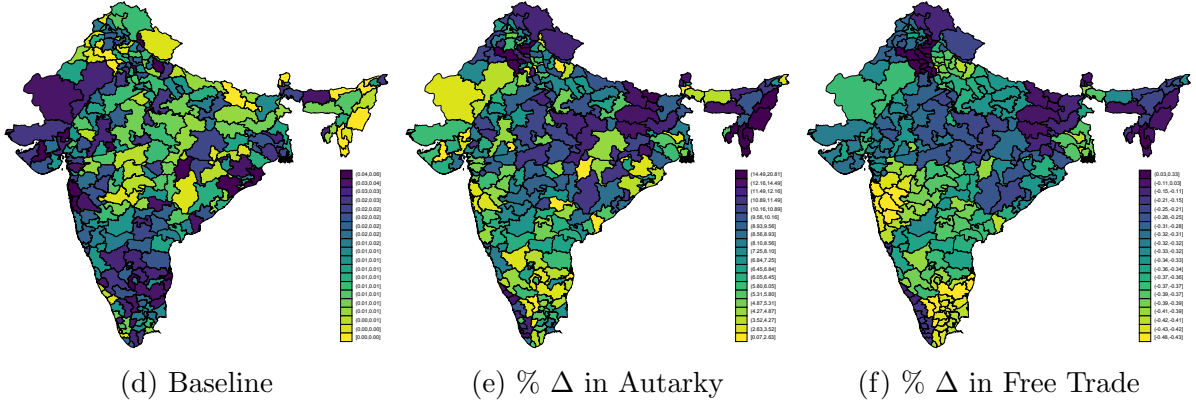
While the previous section explored several counterfactuals such as autarky or free trade, we next study the implications of increasing climate risk in our model. We estimate the share of our model-implied shock probabilities that can be explained by climate-risk related variables such as rainfall or extreme heat. Through the lens our model, these probabilities capture the risk firms assign to each district. However, as discussed above, the risk associated with each region can be due to climate risk, but also other regional characteristics such as infrastructure or governance. To highlight the implications of

Figure 23: Quantitative Results

Panel A: Expected Real Wages



Panel B: Variance of Real Wages



*Note.* This figure shows expected real wages (Panel A) and their variance (Panel B). The left column shows expected real wages and their variance in the baseline calibrated model. In the middle and right columns, the figure shows the percentage changes in expected real wages under the autarky and the free trade counterfactuals relative to the baseline scenario. In the bottom panel, the middle and right figures show the percentage changes in the variance of real wages under the autarky and the free trade counterfactuals relative to the baseline scenario.

changing climate risk, in this section we hold all other sources of risk constant, and double the climate risk of each region relative to the baseline.

## 6 Conclusion

Climate risk is an increasingly important concern worldwide, with large projected economic impacts. Adaptation of firm supply chains to perceived climate risk is an important channel through which economies might adjust to climate risk. Such adaptation has implications for the spatial concentration of economic activity, and regional income. Regions that are low risk but less productive might see increases in their real wages as firms diversify their supply chains.

This paper provided empirical evidence suggesting firm supply chains are structured taking climate risk into account. Our new model of firm supply chain decisions under risk incorporates key patterns we see in the data: firms source the same inputs from multiple locations, and seek drier regions to source inputs even when they are further away. Our calibrated model implies that the impact of climate risk on firm sourcing delivers important implications for economic activity across space. In particular, expected real wages are higher for regions that are less risky. Further, expected real wages decrease under costly trade compared to autarky, as firms diversify their climate exposure by sourcing inputs from less productive and more costly producers. However, the volatility of real wages is lower with the possibility of diversification through supply chains.

## References

- Ackerberg, D. A., K. Caves, and G. Frazer (2015, November). Identification Properties of Recent Production Function Estimators. *Econometrica* 83(6), 2411–2451.
- Antràs, P., T. C. Fort, and F. Tintelnot (2017, September). The Margins of Global Sourcing: Theory and Evidence from US Firms. *American Economic Review* 107(9), 2514–64.
- Balboni, C. (2021, October). In harm's way? infrastructure investments and the persistence of coastal cities. *Mimeo*.
- Balboni, C., J. Boehm, and M. Waseem (2023). Firm adaptation and production networks: Structural evidence from extreme weather events in pakistan.
- Barrot, J.-N. and J. Sauvagnat (2016). Input Specificity and the Propagation of Idiosyncratic Shocks in Production Networks. *Quarterly Journal of Economics* 131(3), 1543–1592.
- Bilal, A. and E. Rossi-Hansberg (2023, June). Anticipating climate change across the united states. Working Paper 31323, National Bureau of Economic Research.
- Boehm, C. E., A. Flaaen, and N. Pandalai-Nayar (2019, March). Input Linkages and the Transmission of Shocks: Firm-Level Evidence from the 2011 Tōhoku Earthquake. *The Review of Economics and Statistics* 101(1), 60–75.
- Boehm, C. E., A. A. Levchenko, and N. Pandalai-Nayar (2020, April). The Long and Short (Run) of Trade Elasticities. NBER Working Paper 27064.
- Borusyak, K., X. Jaravel, and J. Spiess (2021). Revisiting event study designs: Robust and efficient estimation.
- Caliendo, L. and F. Parro (2015, 11). Estimates of the Trade and Welfare Effects of NAFTA. *The Review of Economic Studies* 82(1), 1–44.
- Callaway, B. and P. H. C. Sant'Anna (2020). Difference-in-Differences with Multiple Time Periods. *Journal of Econometrics*.
- Carvalho, V. M., M. Nirei, Y. U. Saito, and A. Tahbaz-Salehi (2021, May). Supply Chain Disruptions: Evidence from the Great East Japan Earthquake. *Quarterly Journal of Economics* 136(2), 1255–1321.
- Caselli, F., M. Koren, M. Lisicky, and S. Tenreyro (2019, 09). Diversification Through Trade\*. *The Quarterly Journal of Economics* 135(1), 449–502.
- Castro-Vincenzi, J. (2024, February). Climate hazards and resilience in the global car industry. *mimeo*.
- Cevallos Fujiy, B., D. Ghose, and G. Khanna (2021). Production Networks and Firm-level Elasticities of Substitution. *Working Paper*.
- Cevallos Fujiy, B., G. Khanna, and H. Toma (2022). The Aggregate Implications of Cultural Proximity. *Working Paper*.

- Cruz, J.-L. and E. Rossi-Hansberg (2023). The economic geography of global warming. Technical report.
- Desmet, K., R. E. Kopp, S. A. Kulp, D. K. Nagy, M. Oppenheimer, E. Rossi-Hansberg, and B. H. Strauss (2021, April). Evaluating the economic cost of coastal flooding. *American Economic Journal: Macroeconomics* 13(2), 444–86.
- Dube, A., D. Girardi, O. Jorda, and A. Taylor (2023). A Local Projections Approach to Difference-in-Differences Event Studies. *NBER Working Paper 31184*.
- Goldberg, P. K. and T. Reed (2023, April). Is the global economy deglobalizing? and if so, why? and what is next? Working Paper 31115, National Bureau of Economic Research.
- Goodman-Bacon, A. (2018, September). Difference-in-Differences with Variation in Treatment Timing. NBER Working Papers 25018, National Bureau of Economic Research, Inc.
- Grossman, G., E. Helpman, and H. Lhuillier (2021). Supply Chain Resilience: Should Policy Promote Diversification or Reshoring? NBER Working Papers 29330, National Bureau of Economic Research, Inc.
- Gu, G. and G. Hale (2022). Climate risks and fdi. *Mimeo*.
- Hsiao, A. (2023). Sea level rise and urban adaptation in jakarta. *Mimeo*.
- Hummels, D., J. Ishii, and K.-M. Yi (2001, June). The Nature and Growth of Vertical Specialization in World Trade. *Journal of International Economics* 54, 75–96.
- Indaco, A., F. Ortega, Taspinar, and Süleyman (2020, 11). Hurricanes, flood risk and the economic adaptation of businesses. *Journal of Economic Geography* 21(4), 557–591.
- Jia, R., X. Ma, and V. W. Xie (2022, July). Expecting floods: Firm entry, employment, and aggregate implications. Working Paper 30250, National Bureau of Economic Research.
- Johnson, R. C. and G. Noguera (2012). Accounting for intermediates: Production sharing and trade in value added. *Journal of International Economics* 86(2), 224 – 236.
- Johnson, R. C. and G. Noguera (2017). A Portrait of Trade in Value-Added over Four Decades. *The Review of Economics and Statistics* 99(5), 896–911.
- Khanna, G., N. Morales, and N. Pandalai-Nayar (2022). Supply Chain Resilience: Evidence from Indian Firms. *Working Paper*.
- Kopytov, A., B. Mishra, K. Nimark, and . Taschereau-Dumouchel, Mathieu (October 5 (2021, October). , endogenous production networks under supply chain uncertainty. *mimeo*.
- Nath, I. (2022). “Climate Change, The Food Problem, and the Challenge of Adaptation through Sectoral Reallocation”. *Mimeo*.
- Pankratz, N. and C. Schiller (2021). Climate change and adaptation in global supply-chain networks. *Mimeo*.

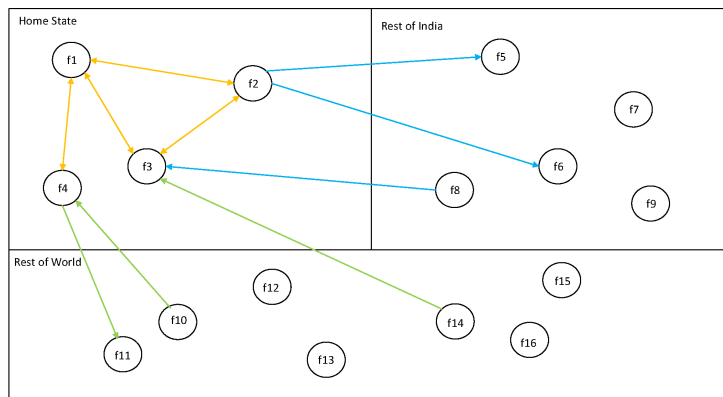
- Sun, L. and S. Abraham (2020). Estimating Dynamic Treatment Effects in Event Studies with Heterogeneous Treatment Effects. Working Paper.
- Yi, K.-M. (2003, February). Can Vertical Specialization Explain the Growth of World Trade? *Journal of Political Economy* 111(1), 52–102.

## Appendix for online publication only

### A Details on the Firm-to-Firm Data

We illustrate a stylized example of our establishment-level networks data in Figure A1. As the diagram shows, we observe all transactions where one node of the transaction is within the state. This includes all transactions between establishments within the state (the yellow lines), any inflows from or outflows to the rest of the country (the blue lines), and all international imports and exports (the green lines).

Figure A1: Stylized Example of Establishment-Level Network



**Notes:** Stylized example of establishment-level data. The upper half represents the country, and the upper left quadrant represents the state in question. The data includes all transactions within the state, and all transactions where one node of the transaction (either buyer or seller) is in the state.

The data report value and quantity of traded items, so we can construct unit values. To do this, we aggregate values and quantities at the four-digit HSN/month/transaction level, and then construct implied unit values. We can then collapse the data at the 4-digit HSN/month level to construct average unit values, the number of transactions between each seller and buyer pair, and total value of the goods transacted. This is the foundation of the firm-to-firm dataset we use in the analysis. Additionally, we can aggregate these data to the buyer level, which we use in our reduced-form section. Table A1 summarizes our primary variables of interest using this dataset.

### B Theory Appendix

#### B.1 Additional Results: Comparative Statics

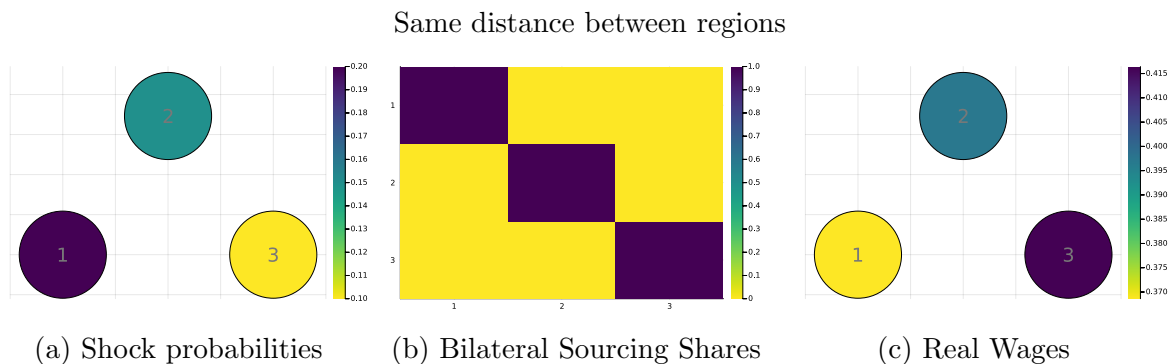
### C Quantitative Appendix

Table A1: Summary Statistics for Main Variables

Outcome	Mean	p25	p50	p75
Separation Rate (%)	30.9	0	16.67	52.78
Entry Rate (%)	74.06	0	50	106.67
Net Separations (%)	-43.12	-70	0	0
Real Input Value (log)	14.91	12.48	14.55	16.96
Real Sales (log)	16.33	13.57	16.05	18.66
Avg. Supplier Size (millions of rupees)	106.42	9.65	34.04	127.49
Avg. Supplier Outdegree	43.04	3.3	10.97	31.99
Share Purch. Lgst. Supplier (%)	52.39	31.06	47.84	71.82
Number Products	12.05	3	7	14
Share Purch. Diff. Prod. (%)	60.19	21.25	72.78	97.81
Supply Chain Depth	32.32	28.15	31.46	36.35
Number Suppliers	12.35	3	7	14
Avg. Distance (km)	486.71	97.13	251.65	712.75
Share Purch. Non-Home State (%)	38.54	0	24.42	78.48

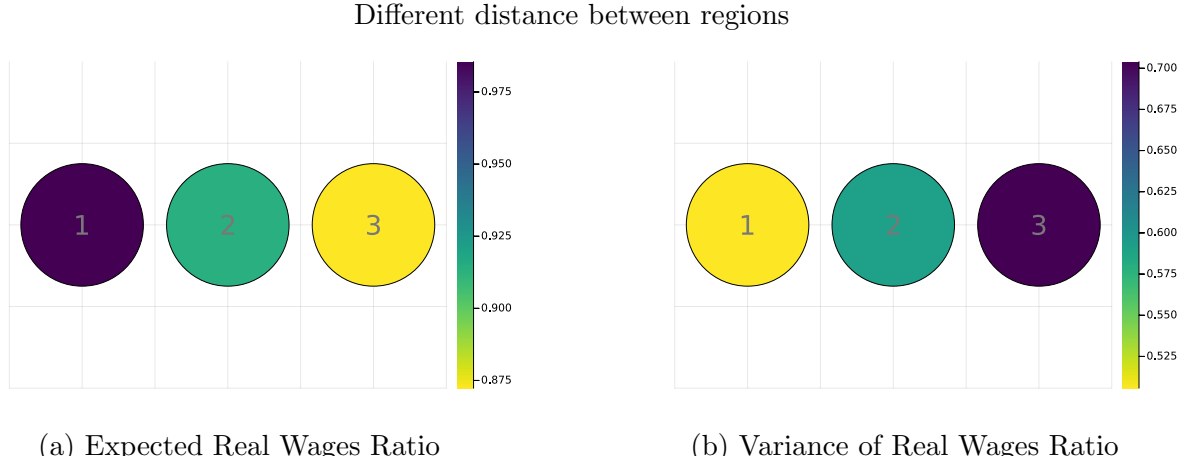
*Note.* We calculate summary statistics for key outcomes to describe the network. Summary statistics calculated in December 2019–February 2020. Number of firms included in calculations: 136,562.

Figure A2: Scenario with heterogeneous risk and infinite trade costs



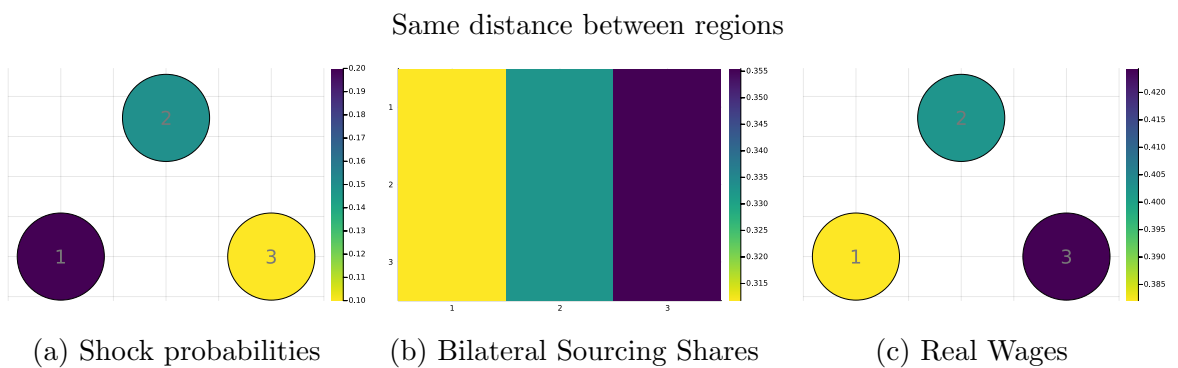
*Note.* This figure presents the case where trade costs are set to infinity and regions are equidistant. The figures in the left panel show the probability that each region is hit by a shock, as well as a visual representation of the geographical location of regions in space. The figures in the middle panel consist of a 3x3 input-output matrix where the buying regions are in the vertical axis and the supplying regions are in the horizontal axis. Each line represents the share of inputs purchased by a buying regions from each supplying region. The right panel present the real wages for each region. The scales are shown to the left of each figure. The case with heterogeneous distance between regions is shown in Figure 14.

Figure A3: Comparison between heterogeneous risk under costly trade and autarky



*Note.* In this figure we plot the expected real wages (left panel) and variance of real wages (right panel) for the scenario with heterogeneous risk and costly trade shown in Figure 12 relative to the scenario with heterogeneous risk and trade autarky shown in Figure 14. The variance of real wages is computed across potential states of the world. In this scenario, regions are equidistant from each other. The scales are shown to the left of each figure. The case with regions in a line is discussed in Figure 15.

Figure A4: Scenario with heterogeneous risk and free trade

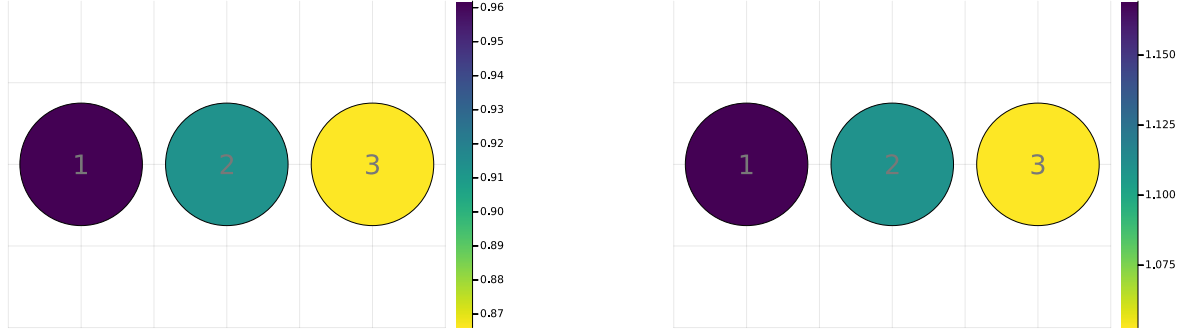


*Note.* This figure presents the case where there are no trade costs. The figure in the left panel show the probability that each region is hit by a shock, as well as a visual representation of the geographical location of regions in space. The figure in the middle panel consist of a 3x3 input-output matrix where the buying regions are in the vertical axis and the supplying regions are in the horizontal axis. Each line represents the share of inputs purchased by a buying regions from each supplying region. The right panels present the real wages for each region. Here, regions are equidistant from each other. The case with heterogeneous distance is in Figure 16. The scales are shown to the left of each figure.

Figure A5: Comparison between costly and free trade

Different distance between regions

Equidistant regions

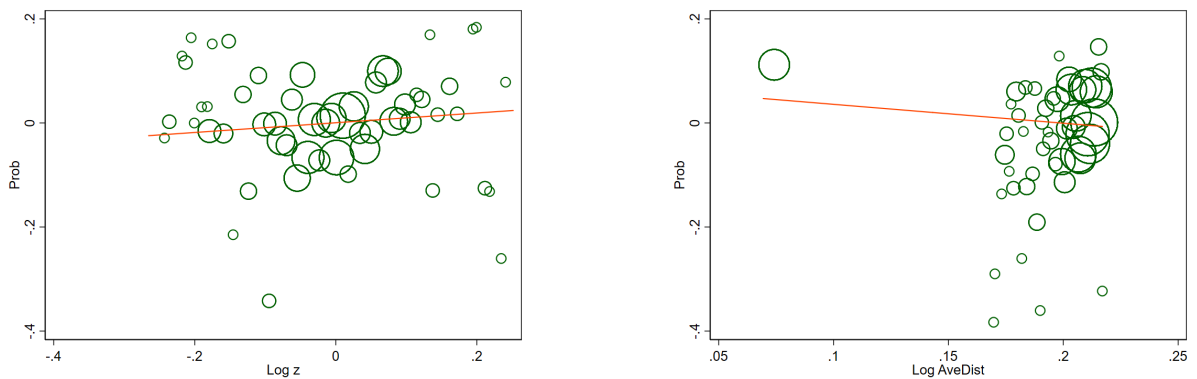


(a) Expected Real Wages Ratio

(b) Variance of Real Wages Ratio

*Note.* In this figure we plot the expected real wages (left panel) and variance of real wages (right panel) for the scenario with heterogeneous risk and costly trade shown in Figure 12 relative to the scenario with heterogeneous risk and free trade shown in Figure 16. The variance of real wages is computed across potential states of the world. Here, regions are equidistant from each other. The case with regions on a line is shown in Figure 17. The scales are shown to the left of each figure.

Figure A6: Model probabilities, Productivities and Distance

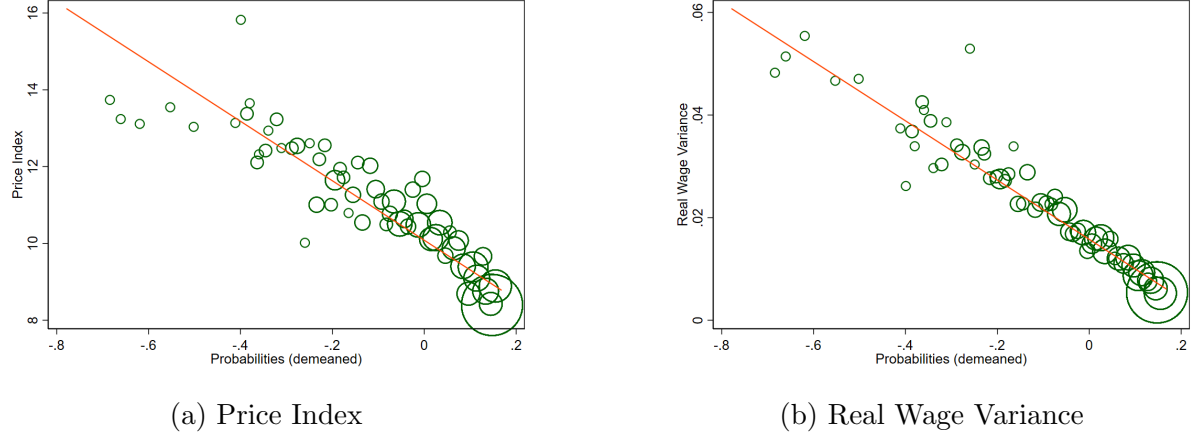


(a) Prob vs Productivities

(b) Prob v Average Distance

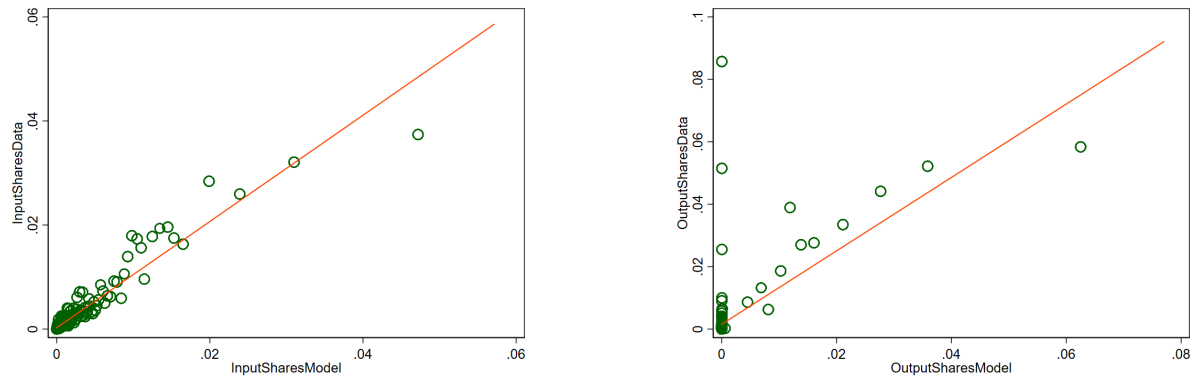
*Note.* In this figure, we plot the estimated probabilities against some observables. In the left panel, we correlate the probabilities with Log(Productivities). In the right panel, we correlate the probabilities with the average distance to the state of our study.

Figure A7: Shock probabilities, Price Indices and Wages



*Note.* In this figure, we plot the model-derived price index (left panel) and real wage variance (right panel) against the estimated shock probabilities.

Figure A8: Low Sourcing Shares: Model vs. Data



*Note.* In this figure, we plot the sourcing shares in the data against the model, but zoom in on low sourcing shares. Figure 20 shows the sourcing shares for the full sample. In the left panel we plot the input sourcing shares. We target average sourcing probabilities from our state's districts to the rest of the districts, but not forcing anything to match the particular sourcing shares of each district. In contrast, the left panel shows the input shares from each district. The right panel shows sales shares, which are entirely untargeted.